The Journal of Physiology

Complex spike clusters and false-positive rejection in a cerebellar supervised learning rule

Heather K. Titley[1], Mikhail Kislin[2], Dana H. Simmons[1], Samuel S.-H. Wang[2] and Christian Hansel[1] (iD)

[1]*Department of Neurobiology, University of Chicago, Chicago, IL, USA*
[2]*Princeton Neuroscience Institute, Princeton University, Princeton, NJ, USA*

Edited by: Ian Forsythe & Maike Glitsch

Key points

- Spike doublets comprise ∼10% of *in vivo* complex spike events under spontaneous conditions and ∼20% (up to 50%) under evoked conditions.
- Under near-physiological slice conditions, single complex spikes do not induce parallel fibre long-term depression.
- Doublet stimulation is required to induce long-term depression with an optimal parallel-fibre to first-complex-spike timing interval of 150 ms.

Abstract   The classic example of biological supervised learning occurs at cerebellar parallel fibre (PF) to Purkinje cell synapses, comprising the most abundant synapse in the mammalian brain. Long-term depression (LTD) at these synapses is driven by climbing fibres (CFs), which fire continuously about once per second and therefore generate potential false-positive events. We show that pairs of complex spikes are required to induce LTD. *In vivo*, sensory stimuli evoked complex-spike doublets with intervals ≤150 ms in up to 50% of events. Using realistic $[Ca^{2+}]_o$ and $[Mg^{2+}]_o$ concentrations in slices, we determined that complex-spike doublets delivered 100–150 ms after PF stimulus onset were required to trigger PF-LTD, which is consistent with the requirements for eyeblink conditioning. Inter-complex spike intervals of 50–150 ms provided optimal decoding. This stimulus pattern prolonged evoked spine calcium signals and promoted CaMKII activation. Doublet activity may provide a means for CF instructive signals to stand out from background firing.

Heather Titley received a Bachelor of Medical Science degree in Physiology from the University of Western Ontario. In 2011, she completed her PhD in Physiology/Neuroscience from the University of Toronto, focusing on the mechanisms of cerebellar motor learning in the vestibulo-ocular reflex. She joined Christian Hansel's laboratory in the Department of Neurobiology at the University of Chicago as a Postdoctoral Scholar. In Chicago, her work focused on synaptic and non-synaptic plasticity in cerebellar Purkinje cells using acute slices and *in vivo* electrophysiology in rodents.

Introduction

A core requirement of supervised learning is an accurate instructive signal. In the Marr–Albus–Ito model of cerebellar learning (Marr, 1969; Albus, 1971; Ito *et al.* 1982), instruction comes in the form of signals from the climbing fibre (CF), which drive long-term depression (LTD) at parallel fibre (PF) to Purkinje cell synapses when the two pathways are coactivated (Ito & Kano, 1982; Ito *et al.* 1982). LTD contributes to a learned output signal via disinhibition of neurons in the cerebellar nuclei, which receive GABAergic input from Purkinje cells. In the absence of CF input, PF stimulation alone triggers long-term potentiation (LTP) (Lev-Ram *et al.* 2002; Coesmans *et al.* 2004). The CF stimulus elicits a voltage transient in the Purkinje cell dendrite and a calcium signal that spreads to fine branchlets and spines contacted by the PF input. The CF-evoked dendritic potential propagates toward the soma where the characteristic complex spike (CS) waveform can be recorded (Davie *et al.* 2008; Ohtsuki *et al.* 2012). Thus, learning at PF synapses constitutes an example of supervised learning, in which CF-evoked CS and their associated dendritic calcium transients act as instructive signals to promote the induction of LTD (Konnerth *et al.* 1992; Wang *et al.* 2000).

However, CF signals are not always informative. CFs fire once per second on average all the time and therefore must fire at times when no salient event has occurred. Spontaneous firing events would therefore potentially add considerable noise to the instructive signal. This problem presupposes that single CF firing events would be sufficient to drive plasticity mechanisms at PF synapses. To date, this has reportedly been the case: single CF stimuli have been found to be sufficient to induce LTD when paired with PF stimulation. However, those studies were performed under non-physiological conditions; specifically, pharmacological block of inhibition and unrealistic calcium and magnesium concentrations. These parameters might affect LTD induction via their effects on calcium signalling. At PF-Purkinje cell synapses, the calcium threshold for LTP is lower than the LTD threshold (Coesmans *et al.* 2004; Piochon *et al.* 2016). Purkinje cell dendrites show calcium-based modulation of excitability and CF coactivation causes supralinear calcium signalling in spines (Wang *et al.* 2000).

An additional source of information in the CF pathway comes from the temporal structure of successive firing events. Structured CF signalling, such as repeated burst firing, may affect key induction signals for plasticity. CFs may fire in high-frequency bursts (Maruta *et al.* 2007), as well as fire at interspike intervals of ∼100 ms, reflecting a natural oscillatory tendency arising in the inferior olive (Lang *et al.* 1999; Ozden *et al.* 2009). Synaptic plasticity also depends on the exact timing of presynaptic and postsynaptic activity. In cerebellar slice recordings, PF and CF co-stimulation has been found to induce LTD with PF–CF intervals ranging from 0 to 250 ms, and sometimes even negative intervals (i.e. CF before PF stimulation) (Ekerot & Kano, 1989; Chen & Thompson, 1995; Bell *et al.* 1997; Wang *et al.* 2000; Coesmans *et al.* 2004; Safo & Regehr, 2008; Sarkisov & Wang, 2008). More recent work has shown that narrow time windows are observed under specific conditions, depending on the area of the cerebellum: in the flocculus, where LTD is induced at a PF–CF interval of 120 ms, and in the vermis, where efficient PF–CF timing intervals for inducing depression at PF synaptic inputs were found to range from 0 to 150 ms, but they were individually tuned for each Purkinje cell (Suvrathan *et al.* 2016) (note that the recordings from the vermis tested short-term, not long-term plasticity). In almost all cases, parametric exploration has been limited to single CF stimuli.

The activity- and timing-dependence of LTD induction under realistic conditions may determine the properties of cerebellum-based learning. However, the timing requirements for synaptic plasticity in brain slices often do not match timing requirements of behavioural learning, raising concerns about the physiological relevance of plasticity (Gallistel & Matzel, 2013). In the case of LTD and cerebellar learning (Wetmore *et al.* 2014), a temporally well-defined teaching signal occurs in delay eyeblink conditioning, in which the unconditioned stimulus (such as an airpuff to the eye) must come after the conditioned stimulus (such as tone or light) by at least 150 ms to allow an anticipatory conditioned response to arise over many trials (Freeman, 2015). This timing does not match some of the reported ranges of effective LTD-inducing time intervals for PF and CF stimulation, suggesting a mismatch between slice and *in vivo* conditions or signals.

In the present study, we aimed to characterize PF-LTD under realistic, physiological activity conditions. We took several steps to design realistic recording conditions. First, we monitored spontaneous and evoked CS activity *in vivo* to identify natural CF activity patterns. Second, we applied these patterns to brain slice recordings. Third, we performed slice experiments and measured synaptic plasticity at near-physiological temperatures (32–34°C), in the absence of blockers of GABA receptors and using realistic $[Ca^{2+}]_o$ (1.2 mM; Nicholson *et al.* 1978) and $[Mg^{2+}]_o$ (1 mM; Ding *et al.* 2016). Finally, we applied high-frequency trains of PF stimuli to mimic granule cell burst firing patterns that have been observed *in vivo* upon sensory stimulation (Chadderton *et al.* 2004). The results of the present study show that, on average, CS recorded upon sensory stimulation *in vivo* occur in ∼20 % of cases in double-pulse clusters and that, in brain slices, clustered CF stimulation is required to induce LTD, with an optimal PF–CF timing interval of 150 ms in crus I.

Methods

Ethical approval

All procedures were performed in accordance with the guidelines of the Institutional Animal Care and Use Committee at the University of Chicago and Princeton University and followed the animal welfare guidelines of the National Institutes of Health. The approved animal protocols used are IACUC 72256 (University of Chicago) and IACUC 1943-19 (Princeton University). All experiments were carried out according to the guidelines laid down by the institutional animal welfare committees and reflected in these approved protocols, as well as the principles and regulations described in Grundy (2015).

Animals

Slice and mouse extracellular recordings were performed on C57BL/6J mice (P25-40; Jackson Laboratory, Bar Harbor, ME, USA). In some experiments, we used TT305/6VA and T305D mutant mice and littermate controls (also on a C57BL/6J background). Optogenetic stimulation was performed using Pcp2-Cre × Ai27 mice on a C57BL/6J background. Whole-cell patch recording *in vivo* was performed using Sprague–Dawley rats (postnatal day 21–30). Both males and females were included in the study.

Slice preparation

Animals were anaesthetized with isoflurane anaesthesia and promptly decapitated, and either the left or right cerebellar hemisphere was removed and placed in cooled artificial cerebral spinal fluid (aCSF) containing (in mM): 124 NaCl, 5 KCl, 1.25 Na_2HPO_4, 2 $CaCl_2$, 2 $MgSO_4$, 26 $NaHCO_3$ and 10 D-glucose, bubbled with 95% O_2 and 5% CO_2. Parasagittal slices (200 µm) of the lateral hemisphere containing crus I were prepared using a VT-1000S vibratome (Leica Microsystems, Wetzlar, Germany) and were kept for at least 1 h at room temperature in oxygenated aCSF. Prior to recording, slices were placed in a bath chamber continuously perfused with aSCF with a lower Ca^{2+} and Mg^{2+} concentration (1.2 and 1 mM, respectively), and glucose was added to adjust the osmolarity of the solution to 295–305 mosmol L^{-1}. The K^+ concentration of 5 mM is higher than that determined during resting states in the cat cerebellum (3 mM) but corresponds to the range from 4 mM to ≤10 mM that is reached when the PF input is stimulated at 5–20 Hz (Nicholson *et al.* 1978). Moreover, throughout the brain, $[K^+]_o$ raises during the shift from sleep to wakefulness from ~3.9 mM to 4.4 mM, with peak values around 5 mM (Ding *et al.* 2016). The concentration of 5 mM $[K^+]_o$ that was selected in the present study therefore reflects K^+ concentrations that are typical for the ionic milieu during activity, which the aCSF should recreate in the otherwise 'silent' slice preparation. The pH of the aCSF used is ~7.4, which is slightly higher than the pH of interstitial fluid in the intact brain (~pH 7.3). The reason for this pH selection in the aCSF is that in brain slices, pH values drop slightly below the pH in the saline, which probably results from the lack of CO_2 clearance by blood flow (Chesler, 2003). The aCSF in the bath was kept at near-physiological temperature (32–34°C) and slices were allowed to acclimate in the solution for at least 20 min prior to recording.

Slice electrophysiology

Patch clamp recordings from Purkinje cell somata located in crus I were performed using an EPC-10 amplifier (HEKA Elektronik, Lambrecht/Pfalz, Germany). Currents were filtered at 3 kHz, digitized at 25 kHz and acquired using Patchmaster software (HEKA Electronik). Patch pipettes (2–5 MΩ, borosilicate glass) were filled with an internal saline containing the following (in mM): 9 KCl, 10 KOH, 120 K-gluconate, 3.48 $MgCl_2$, 10 Hepes, 4 NaCl, 4 Na_2ATP, 0.4 Na_3GTP and 17.5 sucrose (osmolarity adjusted to 295–305 mosmol L^{-1}, pH adjusted to 7.3). Purkinje cells were voltage clamped at a holding potential of –70 mV. Fast and slow capacitances were compensated, and series resistance was partially compensated (60–80%).

To evoke synaptic responses, glass electrodes filled with bath aCSF were placed in the granule layer and upper molecular layer to activate climbing fibres (CFs) and PFs, respectively. Test responses were recorded in voltage clamp mode before and after an induction protocol at a frequency of 0.05 Hz. The LTD or LTP tetanization protocols were applied in current clamp mode. Series and input resistances were monitored throughout the experiments by applying hyperpolarizing voltage steps (−10 mV) at the end of each sweep. Recordings were excluded if the series or input resistances varied by >15% over the course of the experiment. Time course graphs are shown as averages per minute (over three consecutive sweeps). The values were calculated as the mean ± SEM percentage of baseline (calculated from the last 5 min of baseline recording). Final changes in EPSC amplitudes were calculated as the average of last 5 min of recordings (min 31–35) as a percentage of baseline. In some electrophysiology and calcium imaging experiments, we directly compared our higher Ca^{2+}/Mg^{2+} ratio solution (1.2 and 1 mM, respectively) aCSF to the lower Ca^{2+}/Mg^{2+} ratio (2 mM each) aCSF that we used for slicing.

Confocal calcium imaging

Calcium transients were monitored using a LSM 5 Exciter confocal microscope (Carl Zeiss, Oberkochen, Germany) with a 63× Apochromat objective (Carl Zeiss). Calcium

transients were calculated as $\Delta G/R = (G(t) - G_0)/R$, where G is the calcium-sensitive fluorescence (G_0 = baseline signal) of Fluo-5F (300 μM) and R is the calcium-insensitive fluorescence of Alexa 633 (30 μM). The green fluorescence G was excited at 488 nm using an argon laser (Lasos Lasertechnik, Jena, Germany). The red fluorescence R was excited at 633 nm using a HeNe laser (Lasos Lasertechnik). Purkinje cells were loaded with the dyes by diffusion through the patch pipette. The experiments were initiated after the dendrite was adequately loaded with the dyes and the fluorescence at the selected region of interest (ROI) reached a steady-state level (typically requiring ≥30 min). In each recording, the ROI was the spine on a secondary (or higher order) dendritic branch close to the stimulus electrode that responded maximally to synaptic activation.

Surgical preparation for *in vivo* recording

Briefly, mice were anaesthetized with isoflurane (5% for induction; 1.0–2.5% for maintenance), and analgesics (rimadyl, 5 mg kg^{-1}) and lidocaine (50 μL of 2% w/v) were given s.c. An incision was made and skin and connective tissue over the skull were removed. A custom made 'U' titanium headplate was cemented to the skull using dental cement (C&B Metabond; Parkell Inc., Brentwood, NY, USA). A small hole was drilled for a reference electrode in the interparietal bone at the midline. Craniotomies (diameter 1–1.5 mm) were made over the left and right posterior hemispheric cerebellum for extracellular single-unit recordings and optical stimulations. Sterile saline and a fast curing silicone elastomer (Kwik-Sil; World Precision Instruments, Sarasota, FL, USA) were applied on the exposed tissue, and a recording chamber was formed around the craniotomy site using dental cement. Tissue adhesive (Vetbond; 3M, Maplewood, MN, USA) was applied to close the skin around the neck and cement perimeter. Mice were monitored and given postoperative care in their home cages for 5 days after surgery. Next, to acclimate mice to head restraint, they were placed on top of a cylindrical treadmill with their heads fixed for 1 h daily for 3 days; no stimuli were given during this habituation period.

Extracellular recordings and sensory/optogenetic stimulation in mice

After habituation, mice were head-fixed over a freely rotating cylindrical treadmill and the craniotomy site was opened by removing the Kwik-Sil plug and then filled with saline. Single-unit recordings were performed using borosilicate glass electrodes (3–12 MΩ; World Precision Instruments) filled with sterile saline. Purkinje cells were identified by the presence of CS followed by a characteristic pause in simple spikes. Electrical signals were amplified

with a CV-7B headstage and Multiclamp 700B amplifier digitized at 10 kHz with a Digidata 1440A and acquired in pClamp (Molecular Devices, Sunnyvale, CA, USA) in parallel with transistor-transistor logic (TTL) pulses from a signal generator (Master-8; AMPI, Jerusalem, Israel), which was used to synchronize recording and stimulation.

Optical stimulation of cerebellar cortex was performed using a 400 μm diameter optical fibre connected to a fibre-coupled LED and a TTL-controlled driver (Thorlabs, Newton, NJ, USA). Two parameters of the light square pulse were varied from trial to trial: intensity (0.02–5.49 mW) and duration (5–250 ms). Whisker stimulation in awake mice was performed using repeated air puffs (inter-trial interval: 4 s; 100 trials), which were given in a regularly or randomly timed manner using a TTL-controlled pressure injector system (Toohey Spritzer, Toohey, Fairfield, NJ, USA). The air puffs (40 ms and 20 psi) were delivered ipsilateral to the recording site via a small tube (2 mm diameter), approximately placed parallel to the anterior–posterior axis, 10 mm mediolateral and 1 mm anterior to the nose of the mouse.

After the experiments, mice were killed by i.p. injection of euthasol (0.22 ml kg^{-1}) and transcardially perfused with PBS followed by 4% paraformaldehyde for further histological verification of the recording location.

In vivo whole-cell recordings in rats

Sprague–Dawley rats were anaesthetized by an i.p. injection of ketamine (100 mg kg^{-1})/xylazine (10 mg kg^{-1}). The level of anaesthesia was monitored routinely by observing breathing and the responses to noxious stimuli to the hind limbs; additional doses of anaesthetic were given as needed. The animals were placed in a stereotaxic apparatus, and an incision was made along the rostro-caudal midline. A 2 mm craniotomy was made over the crus I area of the cerebellum (3 mm posterior, 4 mm lateral of lambda) and a small hole in the dura was carefully made to expose the brain. The exposed area surface was covered with physiological saline solution or agar (3% in physiological saline).

Whole-cell, patch clamp recordings were made with an EPC-10 amplifier (HEKA Electronik) using the blind-patch method. Borosilicate glass patch pipettes (4–7 MΩ; Sutter Instruments, Novato, CA, USA) containing intracellular saline (see above) and 0.5% biocytin were carefully lowered into the brain, advancing in 2–4 μm steps. After a whole-cell patch was obtained, Purkinje cells were identified by the presence of both simple and CS. Currents were filtered at 3 kHz, digitized at 25 kHz and acquired using Patchmaster software (HEKA Electronik). Spontaneous recordings of Purkinje cell activity (~1–2 min in duration) in current clamp were obtained and analysed. The rats were not allowed

to wake-up from the anaesthesia and were killed (small animal guillotine) at the end of the experiments.

Statistical analysis

Data were analysed using Patchmaster (HEKA Electronik) and Igor Pro (WaveMetrics Inc., Portland, OR, USA). Confocal imaging data were analysed using ZEN (Carl Zeiss). Extracellular data were analysed using custom written packages written in MATLAB (MathWorks Inc., Natick, MA, USA). Statistica (Tibco Software Inc., Palo Alto, CA, USA) was used for statistical analysis. Statistical significance was determined by a two-tailed paired Student's *t* test for within-group comparison of paired events. For comparisons between groups, we used either a Mann–Whitney *U* test (two groups) or the Kruskal–Wallis *H* test with a *post hoc* Dunn's multiple comparison's test (multiple groups). A regression analysis was used to determine correlations. All data are reported as the mean ± SEM.

Results

CS occur in clusters *in vivo*

To monitor CS patterns from intact animals, we first performed whole-cell patch clamp recordings. Recordings were obtained from cerebellar crus I (lateral posterior cerebellum) of anaesthetized rats (Fig. 1*A*). In agreement with previous studies (Bell & Grimm, 1969; Keating & Thach, 1995; Lang *et al.* 1999), we found that CS had irregular firing and featured CS pairs with interspike intervals (ISI) considerably shorter than 1 s (Fig. 1*B*). The mean firing rate of spontaneous CS was 1.24 ± 0.03 Hz (mean ± SEM; 420 CS, $n = 7$ cells, total recording duration: 5.6 min). The interspike interval distribution (Fig. 1*C*) showed a peak near 100 ms, indicative of CS pairs. We found that 12.3% of CS were followed by an interspike interval of ≤150 ms, and 16.5% were followed by an interspike interval of ≤200 ms.

These initial recordings were performed using the whole-cell patch clamp technique, which allows for the acquisition of supra- and subthreshold data without the selection bias that arises from only recording from active neurons (Margrie *et al.* 2002). A caveat of this approach is that we needed to obtain these recordings under anaesthesia to improve the frequency of successful data collection. As a next step, we switched to extracellular recordings, which were performed in awake mice. Spontaneous CS firing occurred at a mean rate of 1.08 ± 0.03 Hz and the coefficient of variation (the ratio between the SD and the mean ISI) was 0.78 ± 0.02, indicating irregular firing activity (2815 CS, $n = 14$ cells). The distribution of CS–CS intervals (Fig. 1*D*) showed the presence of clustering. We observed that 8.8% of CS had an ISI ≤ 150 ms and 13.1% had an ISI ≤ 200 ms. A peak in the ISI histogram at ≤150 ms was visible in 11 out of 14 mouse neurons and in six out of seven rat neurons (Fig. 1*C* and *D*).

Sensory stimulation is known to increase the frequency of CS firing (Ebner & Bloedel, 1981; Bosman *et al.* 2010; Najafi *et al.* 2014*a*; Najafi *et al.* 2014*b*). Enhanced CS responses have been seen after forepaw stimulation (Bloedel & Ebner, 1984), whisker stimulation (Bosman *et al.* 2010) and corneal airpuff (Van der Giessen *et al.* 2008), potentially driven in part by subthreshold rhythmicity of inferior olive neurons (Van der Giessen *et al.* 2008). We examined Purkinje cell responses in mice upon repeated presentations of strong whisker stimulation ipsilateral to the recording site. Air puffs (40 ms at 20 psi) applied to the ipsilateral whisker field increased the probability of at least one CS occurring within 200 ms from the stimulus onset compared to prestimulus baseline in nine out of 11 cells (Fig. 1*E–G*).

It has previously been reported that, in awake mice, a majority of Purkinje cells respond to whisker stimulation within 40 ms, with only a few responding at longer latencies (Bosman *et al.* 2010). Of the 11 cells that we recorded, the latency to first CS was either shorter than 40 ms ('short-latency'; $n = 6$ cells, 35 ± 2 ms, mean ± SEM) (Fig. 1*E*) or longer than 80 ms ($n = 5$ cells, 144 ± 22 ms). Short latency was associated with high response probability and the occurrence of CS doublets. Across all 11 cells (Fig. 1*F* and *G*), the probability of evoking at least one spike was inversely correlated with latency (Spearman's $\rho = -0.81$, different from zero, $P = 0.0015$, two-tailed *r*-to-*z* transformation). Doublet firing (200 ms window) was also inversely correlated with response latency ($\rho = -0.88$, $P = 0.0001$) (Fig. 1*G*) and positively correlated with response probability ($\rho = 0.88$, $P = 0.0001$). In the most responsive neuron (probability 0.94), CS doublets with a spacing of 150 ms or less occurred in 48% of trials, which is the highest fraction observed (Fig. 1*G*). In summary, doublet firing was a prominent feature associated with short-latency sensory responsiveness.

CS doublets have been suggested to be driven by olivocerebellar network effects (Chaumont *et al.* 2013; Witter *et al.* 2013; de Gruijl *et al.* 2014). To probe intrinsic mechanisms of generating CS doublets, we activated the optogenetic probe channelrhodopsin (ChR2) in Purkinje cells ($n = 5$; using Cre mice) for different durations of optical stimulation (5, 25, 100 and 250 ms). Activation of ChR2 in head-fixed mice evoked robust simple spike firing that lasted through the whole stimulus (Fig. 2). Simple-spiking activity inhibits deep nuclei neurons, some of which drive nucleo-olivary projections that are themselves inhibitory. CS arose during 100 and 250 ms light steps, consistent with disinhibition of the inferior
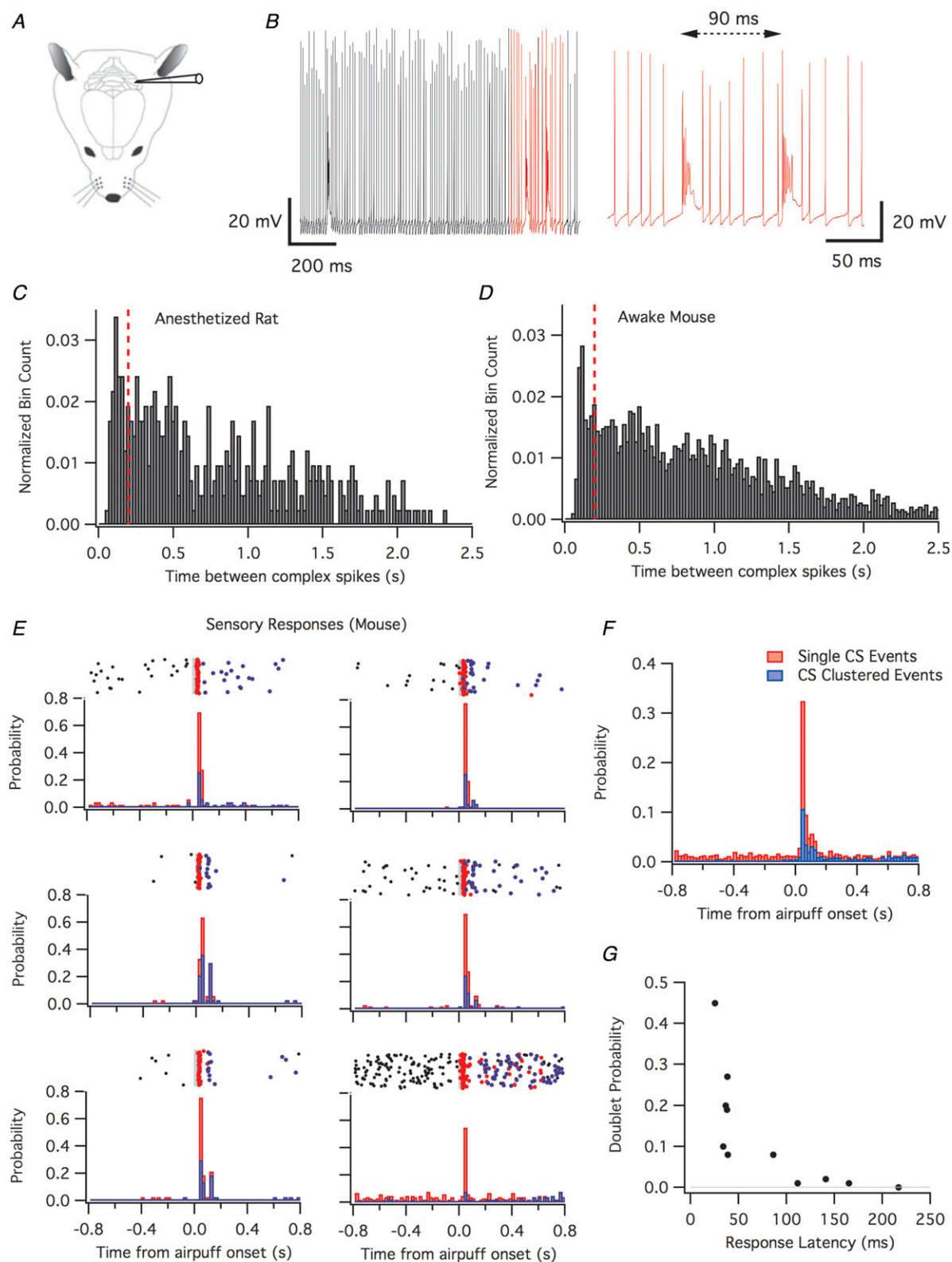
Figure 1. Spontaneous and evoked CS can occur in clusters
A, schematic drawing of a rodent with a recording electrode in crus I of the cerebellum. *B*, example trace of a whole-cell recording taken from an anaesthetized rat (left). Red indicates enlarged region on the right showing two CS with an interspike interval of 90 ms. *C* and *D*, CS interspike intervals in 20 ms bins. Red dashed line shows the 200 ms interval. *C*, binned CS intervals from whole-cell recordings in anaesthetized rats (420 CS from seven

cells). *D*, binned CS interspike intervals recorded extracellularly from awake mice (2815 CS from 14 cells). *E* and *F*, clustered events evoked by whisker stimulation. *E*, CS firing before and after whisker stimulation for six example neurons (out of a total of *n* = 11). Top: CS firing. Red dots represent the first CS to occur after stimulation, whereas blue dots represent the second CS to occur after stimulation. Grey bar indicates the time of whisker stimulation. Bottom: probability of either a single CS event occurring (red) or a CS pair (ISI <150 ms; blue). *F*, probability of a CS occurring (red) and the probability of two CS occurring with an interspike interval of less than 150 ms (blue) upon sensory stimulation (*n* = 11). In (*E*) and (*F*), the bar plots are unstacked. *G*, correlation of the response latency of the first CS with the probability of a CS doublet (*n* = 11).

olive. A post-stimulus rebound phenomenon was also apparent in the form of increased CS probability after the offset of light steps. Rebound CS occurred for all durations of light step, and often occurred within 150 ms of a previously occurring CS (with the first spike in two-spike pairs indicated in red). These results are consistent with the idea (Chaumont *et al.* 2013; Witter *et al.* 2013) that the nucleo-olivary system can generate CS doublets via a mechanism that is enhanced by transient simple-spike firing.

LTD is not induced by single climbing fibre stimuli under near-physiological conditions

We studied long-term depression at PF synapses in cerebellar crus I under near-physiological slice conditions. The external Ca^{2+} concentration was lowered to 1.2 mM (Nicholson *et al.* 1978) and the Mg^{2+} concentration was lowered to 1 mM (Ding *et al.* 2016), with

both being lower than the more commonly used combination of 2 mM $[Ca^{2+}]_o$ and 2 mM $[Mg^{2+}]_o$. GABA inhibition was left intact because we did not add any pharmacological blocker, and we recorded at near-physiological temperatures of 32–34 °C.

We first attempted to induce LTD using single CF stimuli. We used a variety of protocols varying the interval between the first parallel fibre pulse and the CS. Parallel fibres were stimulated eight times at 100 Hz, with the CS occurring at either 0, 70, 100, 150 or 200 ms from the time of the first parallel fibre stimulation (Fig. 3*A*). Although LTD has previously been shown to occur within this wide timing range (Chen & Thompson, 1995; Safo & Regehr, 2008), we failed to see any significant depression under the more realistic ionic and temperature conditions used in the present study (Fig. 3*B*). In three out of the five PF–CS interval protocols (0, 70 and 200 ms), the mean change in EPSC amplitude 30 min after tetanization resulted in a significant potentiation compared to their
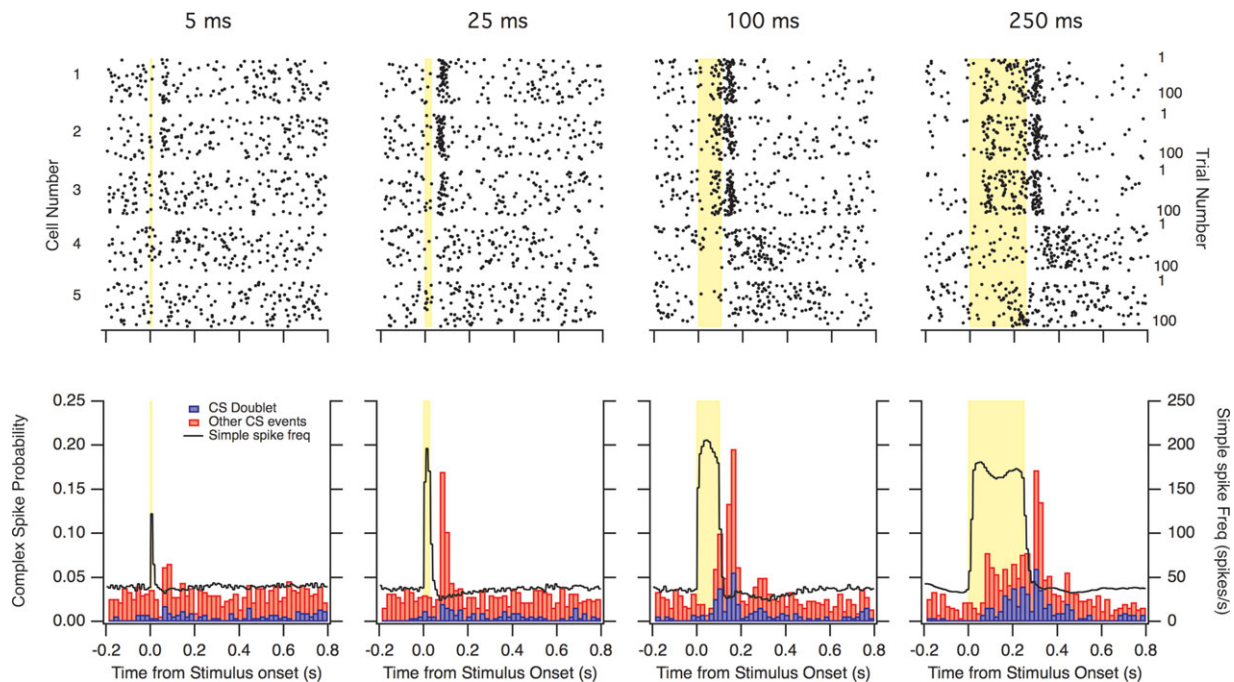
Figure 2. Optogenetic simple spike activation increased CS
Optogenetic stimulation of Purkinje cells with 5, 25, 100 and 250 ms duration (*n* = 5). Top: CS firing during each trial. Bottom: probability of a CS occurring (red) and the probability of CS occurring within 150 ms of each other (blue). Black curve shows the firing rate of simple spikes. Yellow bar indicates the time of stimulation. The bar plots are unstacked.
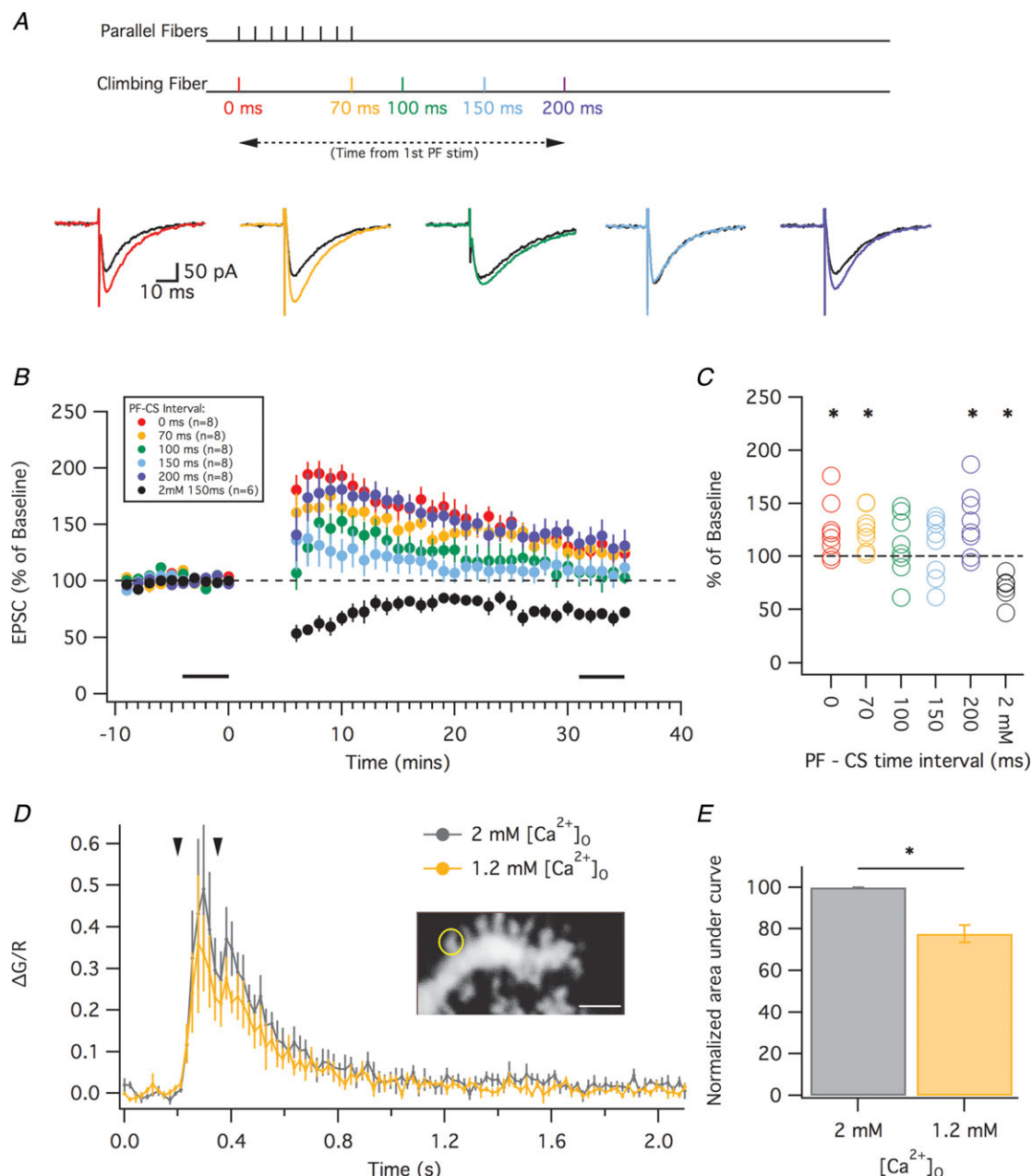
Figure 3. PF-PC LTD failed to induce in more physiological conditions despite the wide range of PF–CS intervals

A, top: schematic depicting timing of parallel and climbing fibre stimulation under the five conditions used. Parallel fibres were stimulated eight times at 100 Hz, with a climbing fibre being stimulated at either 0, 70, 100, 150 or 200 ms from the start of the parallel fibre stimulation. Bottom: example traces showing EPSCs before (black) and after LTD tetanization using a PF–CS timing of either 0 ms (red), 70 ms (orange), 100 ms (green), 150 ms (cyan) or 200 ms (blue). *B*, change in EPSC amplitude (as a percentage of baseline) following the various LTD induction protocols. For comparison, the black trace indicates LTD obtained under non-physiological conditions with 2 mM $[Ca^{2+}]_O$ and with a PF–CS timing interval of 150 ms (in these recordings at room temperature, $GABA_A$ receptors were blocked). Black bars indicate time points that were averaged (baseline and end-point) to calculate changes in EPSC amplitude. *C*, percentage change in EPSC (from baseline) in individual cells using the various PF–CS timing intervals. *D*, calcium transients averaged from Purkinje cell recordings (*n* = 6) during a LTD protocol with the PF–CF interval of 150 ms. Each neuron was recorded in both standard aCSF solution (lower $Ca^{2+}:Mg^{2+}$ ratio, grey) and in the more physiological solution with a higher ratio of Ca^{2+} and Mg^{2+} (yellow). The arrowheads indicate the onset of PF and CF stimulation, respectively. Inset: example of PC dendritic spine filled with Fluo-5F and Alexa 633; the circle outlines the ROI. Scale bar = 2 μm. *E*, the normalized areas of the two curves shown in (*D*) from 0.2 to 1.0 ms. Error bars indicate the SEM. *P < 0.05.

respective baselines (paired *t* test; 0 ms: $124.5 \pm 9.4\%$ SEM, $P = 0.035$, $n = 8$; 70 ms: $125.8 \pm 6.5\%$, $P = 0.005$, $n = 8$; 200 ms: $132.3 \pm 10.8\%$, $P = 0.02$, $n = 8$). In the 100 and 150 ms delay protocols, there was no detectable difference compared to their own baseline (paired *t* test; 100 ms: $110.7 \pm 10.3\%$, $P = 0.33$, $n = 8$; 150 ms: $108.3 \pm 10.1\%$, $P = 0.43$, $n = 8$). Overall, 30 min after tetanization, there were no detectable differences among the protocols (Kruskal–Wallis test, $H = 3.27, 4$; $P = 0.51$). Thus, under near-physiological conditions, LTD was not induced at any of the previously established PF–CS timing intervals. For comparison, under the classical non-physiological conditions (2 mM Ca^{2+} and Mg^{2+}), LTD is successfully induced with a PF–CS interval of 150 ms ($69.9 \pm 5.3\%$; $P = 0.001$, $n = 5$).

Because PF-LTD induction is known to have a higher calcium threshold than LTP (Coesmans *et al.* 2004; Piochon *et al.* 2016), we measured spine calcium transients during the 150 ms PF–CS delay protocol using two different aCSF solutions: the classic aCSF (2 mM Ca^{2+}; 2 mM Mg^{2+}) and our new, near-physiological aCSF (1.2 mM Ca^{2+}; 1 mM Mg^{2+}). We observed a smaller calcium transient with the near-physiological aCSF, suggesting that the lower absolute calcium concentration reduced the response amplitude (Fig. 3*D*). Figure 3*E* shows the area under the curve of the transients normalized to the 2 mM $[Ca^{2+}]_o$ solution. The 1.2 mM $[Ca^{2+}]_o$ solution had a significantly lower area ($77.7 \pm 4.2\%$, $P = 0.003$, $n = 6$, paired *t* test). The reduced calcium transients during the LTD protocol probably explain the lack of depression found after the various LTD protocols and could additionally explain why some protocols even resulted in potentiation.

We tested whether the duration of single CS influenced the ability to induce PF-LTD. It has previously been shown that stimulating the climbing fibre at high frequency (400 Hz) can elongate a CS by increasing the number of spikelets and also that elongated CS have a greater probability of inducing LTD (Mathy *et al.* 2009). By stimulating the climbing fibre at 400 Hz (five stimuli) instead of once, we were able to increase the number of spikelets from 2.8 ± 0.2 to 6.0 ± 0.3 spikelets (Fig. 4*A* and *B*). With a 150 ms PF–CS interval (Fig. 4*C* and *D*, grey), we were still not able to initiate a depression and
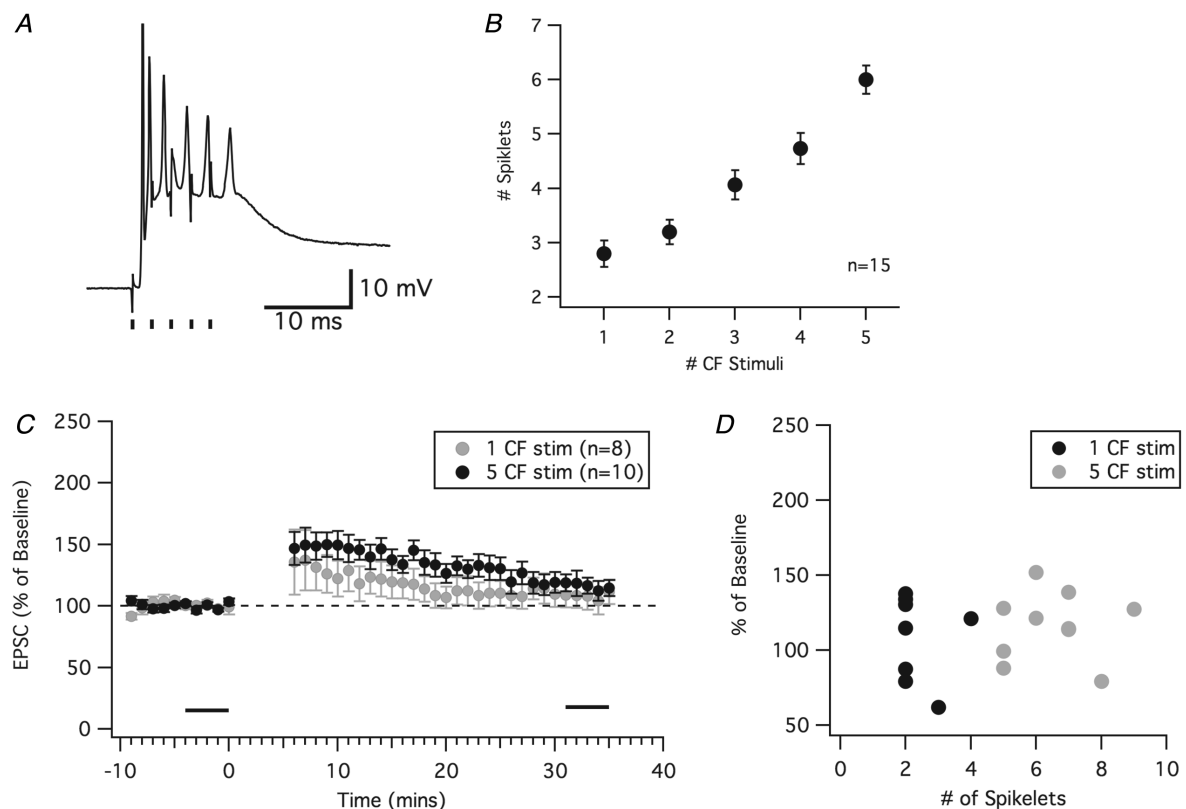
Figure 4. Increasing the number of spikelets in a CS fails to cause LTD
Stimulating the climbing fibre at 400 Hz can elongate a CS by increasing the number of spikelets. *A*, example of a CS with the climbing fibre stimulated five times at 2 ms intervals (black lines). *B*, increase in CS spikelets as the number of climbing fibre stimuli increased. *C*, percentage change in EPSC amplitude (from baseline) following an LTD induction protocol (PF–CS = 150 ms) using either 1-CF stimulation (black) or 5-CF stimulation producing an elongated CS (grey). *D*, percentage change in EPSC amplitude in the individual neurons as a function of the median number of spikelets seen during the 5 min induction protocol. Error bars indicate the SEM.

again observed potentiation compared to its own base-line (116.2 ± 7.1%, *P* = 0.048, *n* = 10, paired *t* test) (Fig. 4*C*). There was no significant difference between the 1-CF stimulation protocol and the 5-CF stimulation protocol (Mann–Whitney *U* test, *P* = 0.69). Furthermore, when plotting the median number of spikelets in a CS for each trial and protocol, there was no correlation of more spikelets leading to a lower EPSC amplitude after a LTD protocol (r^2 = 0.043, *P* = 0.59, *n* = 18) (Fig. 4*D*). Thus, even when increasing the number of spikelets, we were still unable to observe LTD under more physiological conditions.

LTD is successfully induced with CS doublets in a timing-dependent manner

Because we have shown that CS can occur in clusters both spontaneously and when evoked, we aimed to determine whether a cluster of CS was needed for LTD under physiological conditions and, if so, under what time intervals this occurred. For these experiments, we initially used a PF–CS timing interval of 150 ms, the condition that caused the least amount of potentiation under single-CS conditions 30 min after pairing (Fig. 3). To determine whether CS clustering was required for LTD, we added a second CS at 50, 100, 150, 200 or 250 ms after the first CS (Fig. 5*A*). We found that LTD could be successfully induced under more physiological conditions if the second CS occured ≤200 ms from the first. Thirty minutes after the tetanization period, we found that the CS–CS intervals of 50, 100, 150 and 200 ms successfully depressed compared to their baselines (paired *t* test, 50 ms: 72.0 ± 5.8%, *P* = 0.002, *n* = 8; 100 ms: 65.5 ± 5.6%, *P* = 0.004, *n* = 8; 150 ms: 72.9 ± 7.7%, *P* = 0.01, *n* = 8; 200 ms: 84.6 ± 6.4%, *P* = 0.048, *n* = 8) (Fig. 5*C*). Significant LTD was not observed when the CS–CS interval was 250 ms (paired *t* test, 114.8 ± 12.4%, *P* = 0.27, *n* = 8). Furthermore, a groupwise comparison of the double CS groups including the results of the 1-CS condition (compare with Fig. 3) showed a significant difference (Kruskal–Wallis test, *H* = 17.93, 5; *P* = 0.003). *Post hoc* analysis revealed that the 1-CS group was significantly different from the 50 ms (*P* = 0.041), 100 ms (*P* = 0.0097) and 150 ms (*P* = 0.048) groups (Fig. 5*D*). Although the 200 ms CS–CS interval resulted in a depression, it was not found to be significantly different from the 1-CS control group (*P* = 0.36). Thus, we have shown that when the interval from the PF to CS was 150 ms, LTD could be induced if a second complex occured less than 200 ms after the first.

To investigate whether the LTD observed was a result of the second CS and not a difference with respect to greater calcium in the first CS, we measured the area under the CS during the first 50 ms in each CS–CS interval in the PF–CF = 150 ms protocol. There was no difference between the area of the first CS in any of the protocols (Kruskal–Wallis test, *H* = 10.97, 5; *P* = 0.74).

Under near-physiological conditions, we compared the calcium levels during the 1-CS protocol using a PF–CS interval of 150 ms (which failed to result in LTD) with the CS clustering protocols using a CS–CS interval of 50 and 150 ms (which both successfully induced LTD), as well as the failed LTD protocol with the CS–CS interval of 250 ms (Fig. 6). Figure 6*A* shows the calcium transients induced by these four protocols. A second CS can be seen in these calcium transients as a secondary peak, which elongates the elevated calcium signal. We then measured the area under the curves and normalized them to the 1-CS protocol (Fig. 6*B*). We found that the area under the curve resulting from the 50 and 150 ms CS–CS protocols was significantly greater than the area under the curve of the 1-CS protocol (paired *t* tests; 1CS: 100.0%, *n* = 12 compared to 50 ms: 131.3 ± 11.2%, *n* = 12, *P* = 0.017 and 150ms: 126.4 ± 8.7%, *n* = 12, *P* = 0.012). There was no significant difference between the 1-CS protocol to the 250 ms CS–CS protocol (104.5 ± 26.0%, *n* = 12, *P* = 0.3), which can be expected as both protocols resulted in a potentiation. This is consistent with LTD requiring significantly more calcium than LTP in cerebellar Purkinje cells.

We next attempted to evoke LTD with a PF–CS interval of 100 ms, with an added CS either 50, 100, 150, 200 or 250 ms after the first (Fig. 7*A*). Here, we only observed depression when the CS–CS interval was 50 ms (83.8 ± 6.0%, *n* = 8, *P* = 0.03, paired *t* test) (Fig. 7*A*). The 100, 150, 200 and 250 ms groups were all significantly potentiated compared to their baselines (paired *t* test; 100 ms: 118.2 ± 6.5%, *n* = 8, *P* = 0.026; 150 ms: 132.4 ± 13.5%, *n* = 8, *P* = 0.048; 200 ms: 129.9 ± 12.2%, *n* = 8, *P* = 0.044; 250 ms: 132.1 ± 9.4%, *n* = 8, *P* = 0.011). A groupwise comparison including its control 1-CS group (PF–CS = 100 ms) revealed a significant difference among these groups (Kruskal–Wallis test, *H* = 15.7, 5; *P* = 0.0076) (Fig. 7*D*), with the *post hoc* analysis showing the 50 ms CS–CS interval to be significantly different from the 1-CS control (*P* = 0.042).

Finally, we tested whether the addition of a second CS was effective in allowing LTD with a PF–CS interval of 70 or 200 ms. Unlike the 100 or 150 ms PF–CS conditions, the 70 and 200 ms conditions led to potentiation when only one CS was used (Fig. 3). We found that adding a second CS could not induce LTD because we were still unable to cause a depression in either the 70 ms (Fig. 7*B*) or the 200 ms (Fig. 7*C*) PF–CS conditions. When the PF–CS interval was 70 ms, a second CS at any CS–CS interval did not result in depression (Fig. 7*B*) 30 min after the tetanization period. When the CS–CS interval was equal to or greater than 150 ms, we observed a significant increase in the EPSC amplitude compared to its baseline (paired *t* test; 150 ms: 123.5 ± 8.9%, *n* = 6, *P* = 0.04; 200 ms: 146.9 ± 12.9%,

$n = 6$, $P = 0.02$; 250 ms: $126.6 \pm 8.9\%$, $n = 6$, $P = 0.03$). There was no significant increase when the CS–CS interval was 50 ms ($117.2 \pm 6.9\%$, $n = 6$, $P = 0.06$) or 100 ms ($132.9 \pm 17.4\%$, $n = 6$, $P = 0.1$). When compared with the control of one CS, there were no significant differences

between groups (Kruskal–Wallis test, $H = 3.4$, 5; $P = 0.6$) (Fig. 7*E*).

Similarly, when the PF–CS interval was 200 ms, the addition of a second CS also failed to cause a depression at any CS–CS interval (Fig. 7*C*). Indeed, a significant
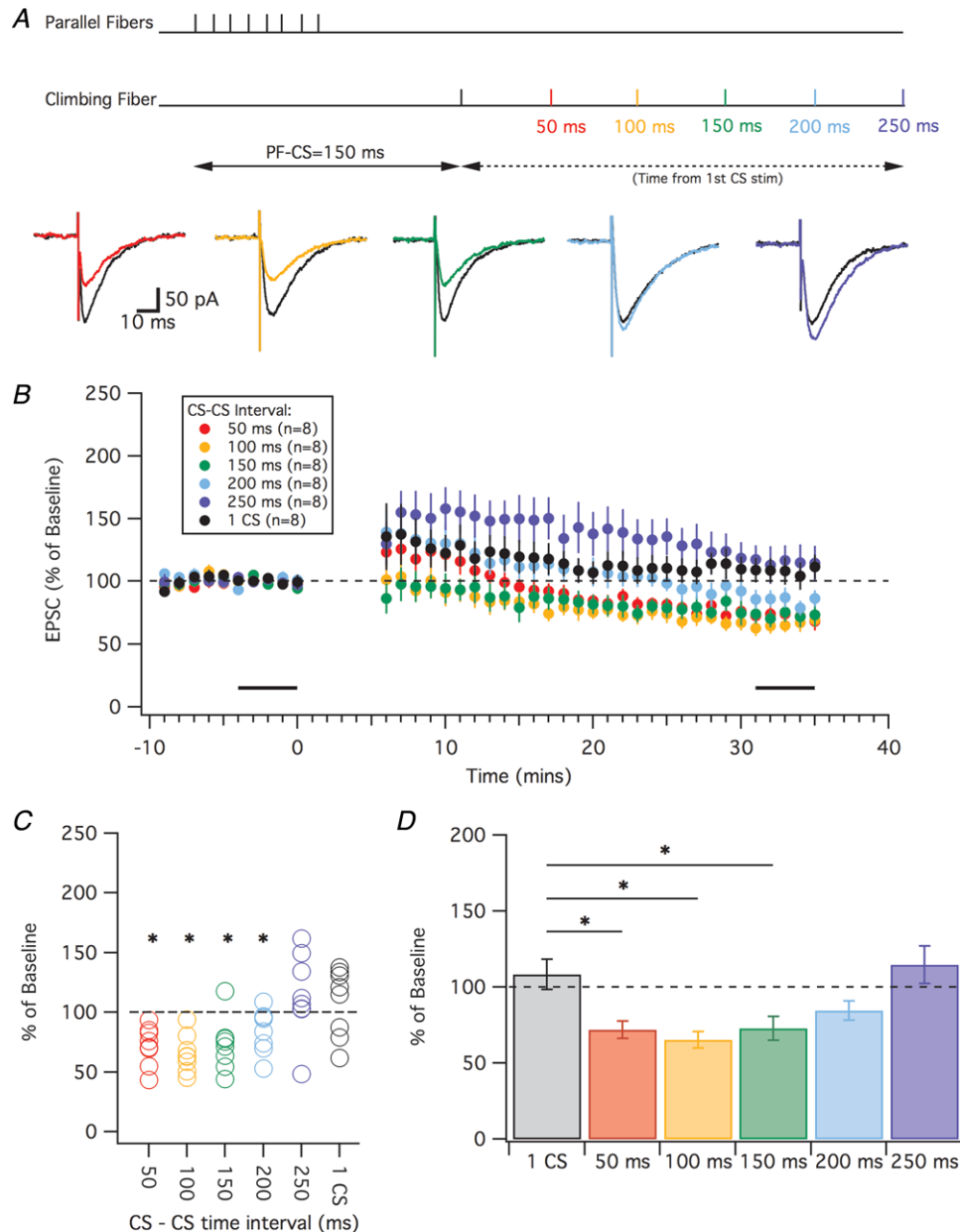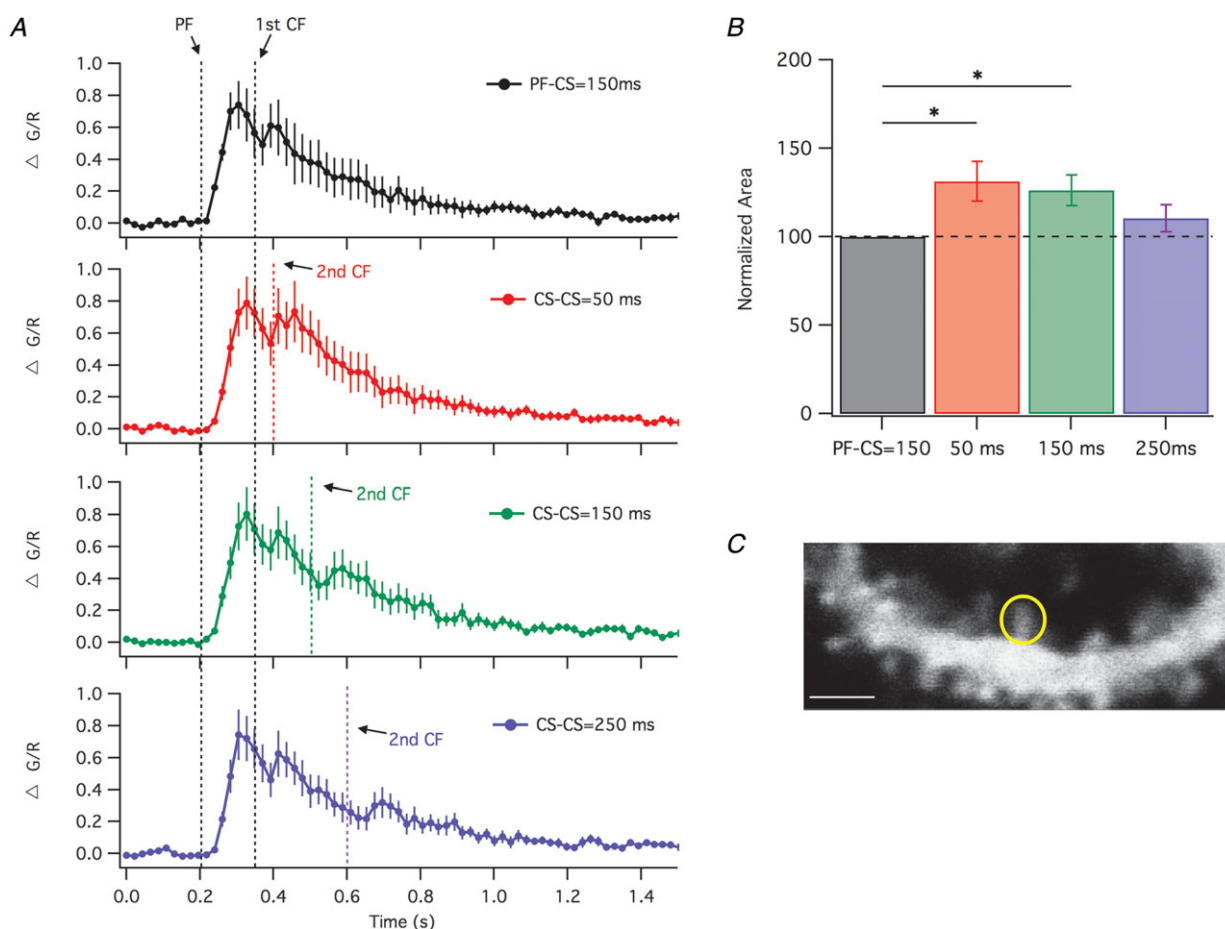

Figure 5. LTD is induced by CS clustering
A, top: schematic depicting timing of the PF–CS = 150 ms with a second CS. Parallel fibres were stimulated eight times at 100 Hz. The climbing fibre was stimulated 150 ms from the start of the PF stimulation and a second CF stimulation occurred with an inter CS interval of either 50, 100, 150, 200 or 250 ms. Bottom: example traces showing EPSCs before (black) and after LTD tetanization using a CS–CS interval of either 50 ms (red), 100 ms (orange), 150 ms (green), 200 ms (cyan) or 250 ms (blue). *B*, change in EPSC amplitude (as a percentage of baseline) following the LTD induction protocols with the various CS–CS intervals. For comparison, the black trace indicates the 1-CS group previously shown in Fig. 3. Black bars indicate time points that were averaged (baseline and end-point) to calculate changes in EPSC amplitude. *C*, percentage change in EPSC (from baseline) in individual cells using the various CS–CS timing intervals. *D*, averaged mean of percentage change in EPSC amplitude of the various CS–CS timing intervals compared to the 1-CS protocol (grey). Error bars indicate the SEM. *$P < 0.05$.

potentiation compared to its baseline occurred when the CS–CS interval was either: 50 ms (123.7 ± 7.1%, $n = 6$, $P = 0.02$), 150 ms (134.4 ± 10.8%, $n = 6$, $P = 0.02$) or 200 ms (125.5 ± 6.5%, $n = 6$, $P = 0.01$). There was no significant change in EPSC amplitude with the CS–CS intervals of 100 ms (121.3 ± 12.5%, $n = 6$, $P = 0.2$) or 250 ms (116.9 ± 6.3%, $n = 6$, $P = 0.1$). When compared with the control group of one CS, there was no significant difference between groups (Kruskal–Wallis test, $H = 2.6$, 5; $P = 0.8$) (Fig. 7F). In summary, LTD induction in crus I required pairs of CS and a PF–CS interval of 100–150 ms (Fig. 7G).

LTD remains dependent on αCaMKII and a higher calcium threshold

Previously, we showed that a key calcium sensor for high frequency (100 Hz) LTD is the autophosphorylation of αCaMKII (Piochon *et al.* 2016). During 100 Hz PF stimulation, higher calcium levels cause αCaMKII to undergo inhibitory autophosphorylation at its 305/306 site, thereby reducing its own activity and increasing the threshold for LTD induction. This shift ensures that LTD activation depends on climbing fibre activity regardless of parallel fibre activation frequency. When the 305/306 site of αCaMKII is blocked (TT305/6VA mice), thereby preventing the auto-inhibition of αCaMKII, the threshold for LTD is lower. Indeed in 2 mM $[Ca^{2+}]_o$ aCSF, we have previously demonstrated that TT305/6VA mice show depression with just parallel fibre burst (LTP) stimulation (Piochon *et al.* 2016). Here, we again show that these mice have a lower threshold for LTD because, in 1.2 mM $[Ca^{2+}]_o$ aCSF and using a 1-CS LTD protocol (PF–CS = 150 ms), TT305/6VA mice (Fig. 8A and B, grey) were able to successfully depress compared to baseline (68.8 ± 4.9%, $n = 5$, $P = 0.003$). When compared with wild-type (WT;

Figure 6. Spine calcium transients depend on stimulus timing
A, calcium transients measured as change of fluorescence ($\Delta G/R$), averaged from recordings of Purkinje cell spines ($n = 12$ cells) from the PF–CS = 150 ms LTD protocol with 1-CS (black), and with 2-CS with a CS–CS interval of 50 ms (red), 150 ms (green) or 250 ms (blue). Black dashed lines represent time of PF and first CF stimulation. Coloured lines represent the second CF stimulation. *B*, area under the curve of the calcium transients (shown in *A*) normalized to the 1-CS response that was recorded from the same cell (top trace in *A*). *C*, example of maximally responding Purkinje cell dendritic spine filled with Fluo-5F and Alexa 633; the circle outlines the ROI. Responses to all four stimuli were recorded from each cell. Error bars indicate the SEM. Scale bar = 2 μm. *$P < 0.05$.

black), there was a significant difference between the groups (Mann–Whitney U test, $P = 0.011$).

We have previously shown that 100 Hz LTD in 2 mM $[Ca^{2+}]_o$ aCSF solution was prevented and resulted in a potentiation in T305D mice, which mimics persistent phosphorylation at the 305 site and prevents Ca^{2+}/calmodulin binding. Here, we show that LTD is prevented in 1.2 mM $[Ca^{2+}]_o$ aCSF in these same mice (Fig. 8C and D, grey). When pairing PF–CS activation (150 ms interval) with CS–CS stimulation (100 ms interval) in T305D mice (Fig. 8C and D, grey), we found that the EPSCs in these mice underwent a significant potentiation compared to baseline ($147.9 \pm 5.4\%$, $n = 5$, $P = 0.0009$). Furthermore, they were significantly different

compared to WT controls (black) (Mann–Whitney U test, $P = 0.0015$). Thus, the autophosphorylation of αCaMKII still appears to control LTD under the conditions of the present study.

With sufficiently strong PF activation, LTD can be induced without a CS (Hartell, 1996). We attempted a variety of protocols that used an additional PF burst in place of the CS (Fig. 9). Regardless of the timing between the PF bursts (70–200 ms) or the number of PF bursts (2 or 3), we failed to observe any significant depression. Figure 9B shows the results of all PF stimulation protocols, with the different intervals used between bursts. In summary, within the range of PF stimulation intensities used, LTD induction required CS activity.
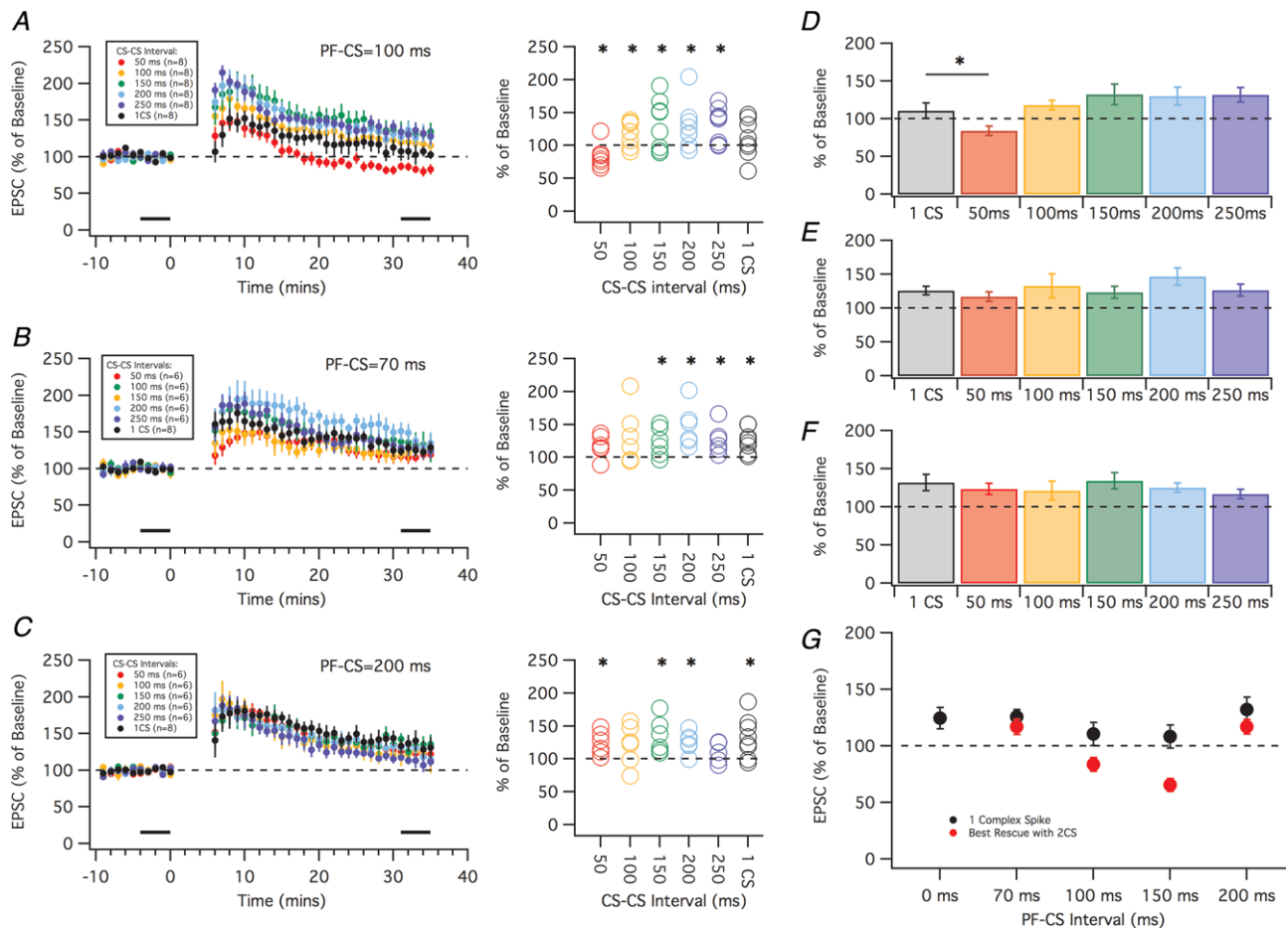
Figure 7. LTD has a preferred timing interval
Results of two CS stimuli at PF–CS interval of 100 ms (A and D), 70 ms (B and E) and 200 ms (C and F). Different CS–CS intervals of either 50 ms (red), 100 ms (orange), 150 ms (green), 200 ms (cyan) or 250 ms (blue) were used to induce LTD. A–C, left: time graphs showing the change in EPSC amplitude (as a percentage of baseline) following the LTD induction protocols with the various CS–CS intervals. For comparison, the black traces indicate the 1-CS group previously shown in Fig. 3. Black bars indicate time points that were averaged (baseline and end-point) to calculate changes in EPSC amplitude. A–C, right: percentage change in EPSC (from baseline) in individual cells using the various CS–CS timing intervals. D–F, averaged mean of percentage change in EPSC amplitude of the various CS–CS timing intervals compared to the 1-CS protocol (grey). G, summary of LTD induction showing precise timing preferences. Black circles: summary of results with LTD protocols with 1-CS across the various PF–CS timing intervals (x-axis). Red circles: best attempt to induce LTD with a protocol with 2-CS. Error bars indicate the SEM. *$P < 0.05$.

Discussion

The main finding of the present study is that, under recording conditions mimicking the physiological ionic milieu, LTD induction at PF synapses requires the co-occurrence of two CF-evoked CS with each PF firing event, and that the timing window for coactivating the PF and the first CF firing event centres around an interval range of 100–150 ms. Our findings demonstrate that the lower calcium concentration used in the present study makes it more difficult to induce LTD and they also suggest that the occurrence of LTD *in vivo* will be restricted to specific activity patterns. Although possibly not an exclusive condition for the induction of LTD, the preferred pattern of repeated CS shows that prolonged calcium signalling, and with it the prolonged presentation of the instructive signal, constitutes a favourable physiological trigger for LTD.

CS clusters and single CS as distinct instructive signals

Our LTD experiments suggest that individual CS are false positives in the context of supervised learning, with CS cluster activity comprising a means to reject these events. The finding that an efficient CF instructive signal for LTD induction requires CFs to fire twice in succession leads to the question of the nature and function of single firing events. Our *in vivo* recordings support previous studies reporting that whisker air puff stimulation elicits well-timed CF responses in Purkinje cells (Bosman *et al.* 2010; Najafi et al. 2014*a*, 2014*b*; Kitamura & Häusser,
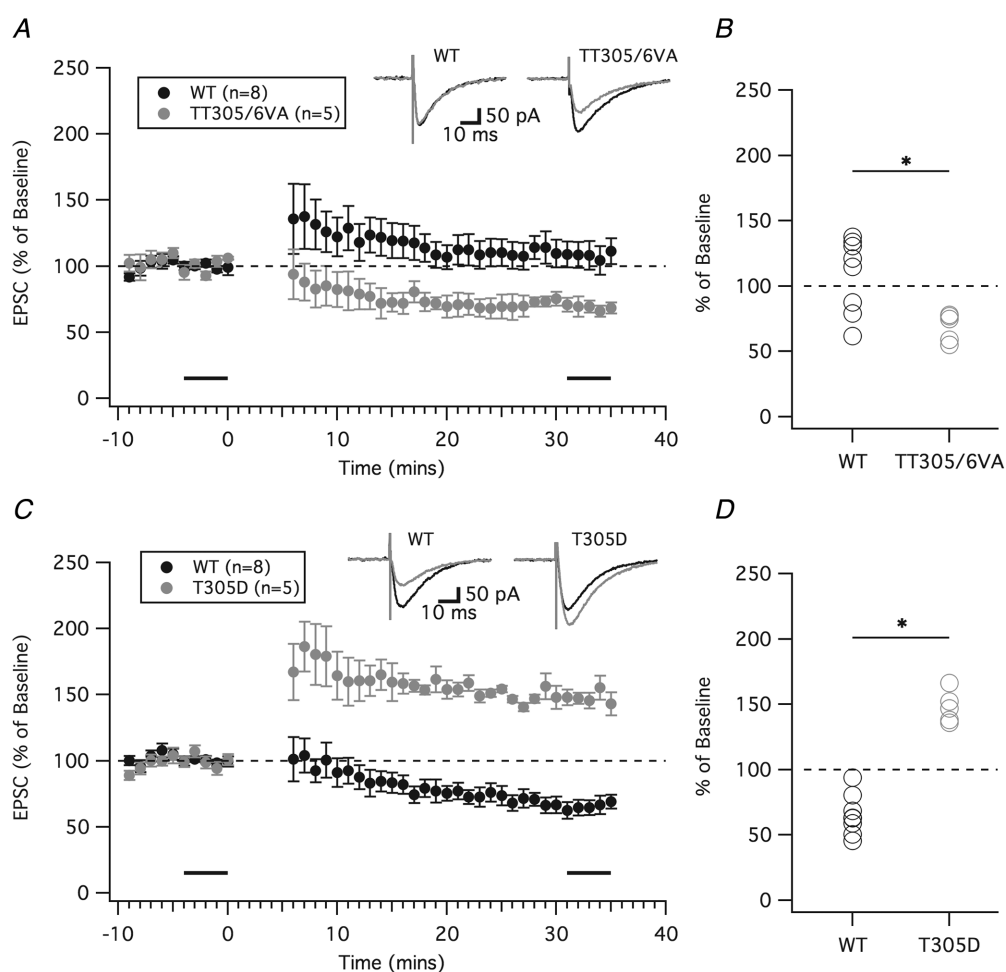

Figure 8. LTD depends on αCaMKII
A and *B*, 1-CS LTD was successful in TT305/6VA mice. *A*, time course of EPSC amplitude (percentage of baseline) in αCaMKII TT305/6VA mice (grey) in the 1-CS LTD protocol (PF–CS = 150 ms) compared to WT mice (black). *B*, percentage change in EPSC amplitude in each individual cell after LTD tetanization. Black bars indicate time points that were averaged (baseline and end-point) to calculate percentage changes in EPSC amplitude. *C* and *D*, 2-CS failed to induce LTD in T305D mice. *C*, time course of EPSC amplitude (percentage of baseline) in αCaMKII T305D mice (grey) with the 2-CS LTD protocol (PF–CS = 150 ms, CS–CS = 100 ms) compared to WT mice (black). *D*, percentage change in EPSC amplitude in each individual cell after LTD tetanization. Error bars indicate the SEM. *$P < 0.05$.

2011; Brown & Raman, 2018). These are responses to salient stimuli that qualify as unconditioned stimuli in motor learning, and therefore act as potential instructive signals in supervised learning. Within this group of evoked responses, ~20% of firing events show doublets with inter-CS intervals of less than 150 ms, whereas ~10% of spontaneous firing events are doublets. Upon sensory stimulation, the percentage of doublets can be substantially higher, reaching up to ~50% in those neurons that reliably respond to air puff stimulation with at least one CS, and do so at short latency. Because, under our slice experimental conditions, doublets drove LTD and single CS could drive LTP, these measurements suggest that evoked activity can provide efficient instruction for LTD, whereas spontaneous activity does not. Although we have not tested the plasticity consequences of mixed multiple and single CS responses, it is possible that the CS can drive bidirectional plasticity (i.e. LTD or LTP) depending on the type of response that is evoked. It should also be noted that single CF firing events may still lead to transient decreases in Purkinje cell simple spike firing output, thereby leading to a transient adaptive response. CS doublets have also been reported in other studies both after air puff unconditioned stimuli (Van der Giessen *et al.* 2008) or in response to conditioned stimuli after eyeblink conditioning (Ten Brinke *et al.* 2019). The occurrence rate of doublets varies greatly under these conditions and probably depends on the exact cerebellar region of recording, the nature of the stimuli used, and the attentional state of the animal and its expectance of incoming stimuli.

The prevalence of CS doublets places a limit on possible roles of oscillatory mechanisms in neural coding. The inferior olive's natural rhythmicity was once suggested to provide a motor clock to initiate muscle contraction and movement (Lamarre, 1984; Llinás, 1984; Welsh *et al.* 1995; Llinás, 2011). This clock hypothesis was originally motivated by observations of tremor associated with continuous, rhythmic olivary activity at 10 Hz under pathological conditions (Gautier & Blackwood, 1961). Such a rhythm can be driven by intrinsic mechanisms that are prominent in anaesthetized animals and in brain
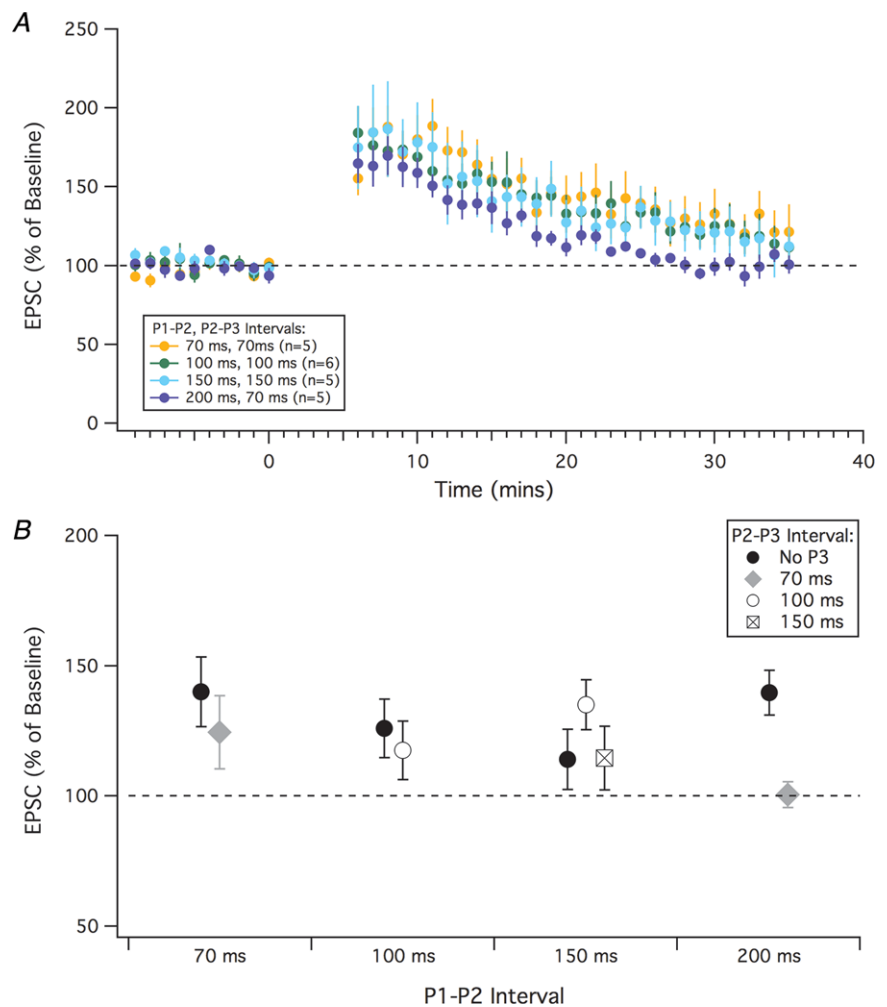
Figure 9. LTD is not induced by parallel fibre stimulation alone
EPSC amplitude (percentage of baseline) after different LTP protocols mimicking parallel fibre bursts instead of a CS. A burst of eight parallel fibre stimuli at 100 Hz (P_1) was used at different timing intervals (time between first and second parallel fibre stimulation) and various repeats (two or three times). *A*, time courses of selected protocols showing the change in EPSC amplitude over time following an LTP induction protocol with various PF burst intervals. *B*, averaged percentage change in EPSC amplitude showing all LTP protocols attempted with various parallel fibre stimulation timing intervals (e.g. P1–P2 and P2–P3). Error bars indicate the SEM.

slices. However, periodicity of CS firing has generally not been observed in awake mammals (Thach, 1968; Armstrong, 1974; Oscarsson, 1980), including a systematic search during cued wrist movements in monkeys (Keating & Thach, 1995). Keating & Thach (1995) also observed rebound firing of a second CS, as have later studies of movement (Chaumont *et al.* 2013, Witter *et al.* 2013, De Gruijl *et al.* 2014) and sensory responses after learning (ten Brinke *et al.* 2019). We found that doublets can also occur spontaneously, as well as under sensory stimulation, although we did not observe ongoing, periodic CS firing under these conditions. Our optogenetic experiments are consistent with the idea that such doublets rely on nucleo-olivary feedback mechanisms (Chaumont *et al.* 2013; Witter *et al.* 2013). In summary, to date, the effect of rhythmic tendencies in olivary activity is not prolonged sequences, but rather doublets, as might occur in a damped oscillator.

CS clustering is required for LTD induction

Initial studies on the requirement for CF coactivation in LTD induction conceptualized the CF as an instructive signal operating in a yes/no mode to drive supervised learning (Ito *et al.* 1982; Coesmans *et al.* 2004). Our observation that, under near-physiological recording conditions, single CF pulses are ineffective and double pulses are required shows that a binary yes/no framework is an insufficient description of CF firing events. The CF pathway has previously been shown to have plasticity consequences that are not fully captured by the presence or absence of a CS, as suggested previously (Eccles *et al.* 1964). Important additional parameters include CF plasticity (Hansel & Linden, 2000), variations in the number of spikes propagated along the fibre itself (Maruta *et al.* 2007; Mathy *et al.* 2009; Najafi *et al.* 2014*b*), variations in spikelet activity (Coesmans *et al.* 2004; Mathy *et al.* 2009) and modulation of the CF response in Purkinje cell dendrites by inhibition (Rowan *et al.* 2018). Although the studies cited above do show that modulations of the instructive signal can alter its impact on the plasticity outcome, they allow the possibility that the instructive signal must reach some all-or-none threshold to induce plasticity. In the present study, we found that, under our experimental conditions, a central requirement of LTD induction was the presence of multiple CS.

An earlier study (Bouvier *et al.* 2018) reported LTD induction by two CS separated by 100 ms. In those experiments, the first CS coincided with granule cell activity and was interpreted as a perturbation signal, whereas the second, delayed CS acts as an error signal, with an overall PF–CF stimulus duration lasting 100 ms, a pattern resembling classic PF–CF coactivation protocols. Our work, which explored a range of timing conditions, demonstrates that a PF–CF–CF sequence to trigger

maximal LTD spans a longer interval, 200–400 ms. In our recordings, we observed that a prolongation of the waveform of a single CS by delivering five pulses to the CF input at 400 Hz does not promote LTD. This finding shows that elevated dendritic spike activity over hundreds of milliseconds constitutes the optimal trigger for LTD induction.

We also show that, under near-physiological recording conditions, the repetitive CF stimulation cannot be replaced with equally timed PF burst stimulation, as was previously shown under classic experimental conditions (Hartell, 1996; Han *et al.* 2007). However, our data do not generally exclude the possibility that sufficiently intense PF activity alone can induce LTD (note the similarity of PF burst signals amplified by intrinsic plasticity with CS) (Ohtsuki *et al.* 2012; Ohtsuki & Hansel, 2018).

Prolonged calcium signalling facilitates the activation of CaMKII

The aCSF used in the present study contained a $[Ca^{2+}]$ of 1.2 mM (instead of the classically used concentration of 2 mM) and a $[Mg^{2+}]$ of 1 mM (instead of 2 mM). These values were based on measures of $[Mg^{2+}]_o$ from the intact brain (Ding *et al.* 2016), as well as measures of $[Ca^{2+}]_o$ from the cerebellum (Nicholson *et al.* 1978) and neocortex (Heinemann *et al.* 1977). Despite the higher Ca^{2+}/Mg^{2+} ratio in this updated aCSF recipe, synaptically evoked calcium transients in dendritic spines were smaller, probably resulting from the lower absolute $[Ca^{2+}]_o$. As the calcium threshold for PF-LTD is higher than the threshold for LTP (Coesmans *et al.* 2004; Piochon *et al.* 2016), the reduced calcium influx will lower the probability for LTD induction and instead result in LTP, as we indeed observed. The 'rescue' of LTD with prolonged CS activity was associated with a significant increase in spine calcium transients. The observation that is duration of the $[Ca^{2+}]_i$ elevation that increases (and not the amplitude) is consistent with the leaky integrator model of calcium signalling in LTD induction, which states that the calcium threshold for LTD becomes lower with a longer presentation of the calcium elevation (Tanaka *et al.* 2007; Chimal & De Schutter, 2018). Similarly, it has been shown that sustained elevation of calcium lowers the calcium threshold for the dendritic release of endocannabinoids (Brenowitz *et al.* 2006). The relatively long interval between the two CF pulses (50 to 200 ms) that leads to LTD induction when the interval between PF and CF stimulus onset is 150 ms suggests that there are additional factors that determine the permissive time windows for LTD induction. One candidate is the kinetics of calcium-binding proteins, such as calbindin and parvalbumin, which enable spread of calcium by buffered diffusion and allow for the activation of calmodulin into adjacent dendritic shafts and even into

neighbouring spines (Schmidt *et al.* 2003; Santamaria *et al.* 2006; Schmidt *et al.* 2007).

Our experiments identify calcium/calmodulin-dependent protein kinase II (CaMKII) as a calcium sensor that benefits from the prolonged calcium transient (Chimal & De Schutter, 2018). LTD induction requires the activation of αCaMKII (Hansel *et al.* 2006). CaMKII suppresses the activation of protein phosphatase 2A via negative regulation of phosphodiesterase 1 and subsequent disinhibition of a cGMP/protein kinase G pathway, thus promoting LTD (Kawaguchi & Hirano, 2013). The inhibitory autophosphorylation of CaMKII at Thr305/306 (Elgersma *et al.* 2002), which may result from calcium/calmodulin binding and subsequent dissociation, possibly as a result of calcium transients that are too low in amplitude and/or do not last sufficiently long (Coultrap & Bayer, 2012), prevents cerebellar LTD and instead results in LTP (Piochon *et al.* 2016). Our finding that LTD is restored upon PF coactivation with a single CF pulse in TT306/6VA mice, in which Thr305 and Thr306 are replaced by the non-phosphorylatable amino acids valine and alanine, respectively, demonstrates that LTP results from this protocol under near-physiological recording conditions because of the self-inhibition of CaMKII. The ability of inhibitory CaMKII autophosphorylation to prevent LTD is shown by the finding that PF-coactivation with two CF pulses results in LTP in phosphomimetic T305D mice, in which Thr305 is replaced by aspartate, preventing calcium/calmodulin binding.

Timing requirements of LTD and learning

For many years, LTD was widely accepted as a cellular mechanism underlying forms of cerebellar learning, ranging from delay eyeblink conditioning (Ito & Kano, 1982; Ito *et al.* 1982) to eye movement adaptation. Moreover, optogenetic inhibition of AMPA receptor endocytosis and LTD has been found to prevent cerebellar motor learning (Kakegawa *et al.* 2018). However, a role for LTD in cerebellar learning has been questioned by findings that pharmacological or genetic blockade of LTD does not cause learning impairment (Welsh *et al.* 2005; Schonewille *et al.* 2011). These claims of mismatches between cellular and behavioural learning outcome have been tempered by the demonstration that LTD might be present under some induction conditions but not others (Yamaguchi *et al.* 2016). *In vivo* observations support a critical role of CF signalling in learning. Continuous CF coactivation at a rate of four pulses per second triggers LTD in decerebrate rabbits (Ito *et al.* 1982) and LTD is also observed in awake mice upon sensory input (whisker) stimulation resulting in PF and CF activation (Marquez-Ruiz & Cheron, 2012). However, it has been reported more recently that associative learning cannot be triggered by single pulse CF co-stimulation (Rasmussen *et al.* 2013) and instead requires intervals between the conditioned and unconditioned stimuli of 150 ms or longer (Wetmore *et al.* 2014). Our findings suggest the possibility that such discrete-trial experiments might also be conducted with multiple CS per trial and a PF–CF time interval in the range of 100–150 ms, comprising conditions that are required to trigger LTD under realistic recording conditions.

In an alternative view of the ability of CS features to drive learning, Yang & Lisberger (2014) demonstrated, using single-unit extracellular recordings, that the number of spikelets in CS waveforms is correlated with learning, leading to the suggestion that CS waveform may be a specific trigger for plasticity mechanisms. An increased spikelet number could be driven by high-frequency CF activation at timing intervals smaller than the duration of a CS. It could also be driven by co-occuring mossy fibre activity (Najafi *et al.* 2014*a*,*b*). We have shown that optogenetic activation causing simple spike firing can also lead to CS-doublet generation. Therefore, these two features of CS responses (i.e. doublet firing and increased spikelet number) may be correlated phenomena. Testing whether this is true will help determine whether these views of effective learning are related.

Remaining caveats centre on the incomplete emulation of other *in vivo* conditions, including neuromodulation, as well as the naturally occurring amount and pattern of mossy fibre/granule cell and climbing fibre activity. These gaps might contribute to remaining mismatches, such as the observation that we did not observe LTD induction at a PF–CF interval of 200 ms, whereas associative learning works well in this longer interval range. The details of mismatch at longer intervals could be explained by the involvement of multiple plasticity mechanisms in learning, some of which are triggered at longer time intervals. Indeed, it has been suggested that cerebellar motor learning rests on multiple mechanisms at multiple brain sites (Hansel *et al.* 2001; Freeman & Steinmetz, 2011; Gao *et al.* 2012; Titley *et al.* 2017; Titley *et al.* 2018).

Beyond timing-dependent LTD, Purkinje cells also express a strong cell-autonomous form of plasticity, and learning can occur without temporally patterned synaptic input (Johansson *et al.* 2014). Intrinsic excitability changes may aid in driving memory formation, with synaptic plasticity serving to determine the information content by individual neurons (Titley *et al.* 2017). In cerebellar learning, this equates to a scaling of synaptic input weights depending on whether PF synapses contribute to the occurrence of an error. Synthesis of timing-dependent and timing independent learning mechanisms will require behavioural experiments that go beyond single-stimulus tests of learning such as eyeblink conditioning, which only test for the occurrence of a discrete well-timed response.

Our findings have several implications for cerebellar learning. First, the majority of CS that are fired do

not contribute to LTD induction and the requirement for doublets (or more) of CS acts as a noise reduction mechanism that allows only salient instructive signals to drive plasticity. Second, the difficulty of inducing LTD emphasizes the role of repetitive PF activation, which by itself induces LTP, leading to bidirectional plasticity, as found in adaptive filter models of cerebellar learning (Dean *et al.* 2010). Third, it requires the re-evaluation of predictions regarding cerebellar learning. For example, recent observations identify conditioned stimulus-evoked CS as a hallmark of Purkinje cells that change the spike firing output in eyeblink conditioning (Ohmae & Medina, 2015; Ten Brinke *et al.* 2015). It is possible that the combination of PF activity followed by a conditioned stimulus-evoked and an unconditioned stimulus-evoked CS, and/or double conditioned stimulus-evoked CS responses (Ten Brinke *et al.* 2019), are well suited for inducing LTD.

References

Albus JS (1971). A theory of cerebellar function. *Math Biosci* **10**, 25–61.

Armstrong DM (1974). Functional significance of connections of the inferior olive. *Physiol Rev* **45**, 358–417.

Bell CC & Grimm RJ (1969). Discharge properties of cerebellar Purkinje cells recorded with single and double microelectrodes. *J Neurophysiol* **32**, 1044–1055.

Bell CC, Han VZ, Sugawara S & Grant K (1997). Synaptic plasticity in a cerebellum-like structure depends on temporal order. *Nature* **387**, 278–281.

Bloedel JR & Ebner TJ (1984). Rhythmic discharge of climbing fibre afferents in response to natural peripheral stimuli in the cat. *J Physiol* **352**, 129–146.

Bosman LWJ, Koekkoek SKE, Shapiro J, Rijken BFM, Zandstra F, Van der Ende B, Owens CB, Potters J-W, De Gruijl JR, Ruigrok TJH & De Zeeuw CI (2010). Encoding of whisker input by cerebellar Purkinje cells. *J Physiol* **588**, 3757–3783.

Bouvier G, Aljadeff J, Clopath C, Bimbard C, Ranft J, Blot A, Nadal J-P, Brunel N, Hakim V & Barbour B (2018). Cerebellar learning using perturbations. *eLife* **7**, e31599.

Brenowitz SD, Best AR & Regehr WG (2006). Sustained elevation of dendritic calcium evokes widespread endocannabinoid release and suppression of synapses onto cerebellar Purkinje cells. *J Neurosci* **26**, 6841–6850.

Brown ST & Raman IM (2018). Sensorimotor integration and amplification of reflexive whisking by well-timed spiking in the cerebellar corticonuclear circuit. *Neuron* **99**, 564–575.

Chadderton P, Margrie TW & Häusser M (2004). Integration of quanta in cerebellar granule cells during sensory processing. *Nature* **428**, 856–860.

Chen C & Thompson RF (1995). Temporal specificity of long-term depression in parallel fiber-Purkinje synapses in rat cerebellar slice. *Learn Mem* **2**, 185–198.

Chesler M (2003). Regulation and modulation of pH in the brain. *Physiol Rev* **83**, 1183–1221.

Chimal CGZ & De Schutter E (2018). Ca2+ requirements for long-term depression are frequency sensitive in Purkinje cells. *Front Mol Neurosci* **11**, 438.

Chaumont J, Guyon N, Valera AM, Dugue GP, Popa D, Marcaggi P, Gautheron V, Reibel-Foisset S, Dieudonne S, Stephan A, Barrot M., Cassel JC, Dupont JL, Doussau F, Poulain B, Selimi F, Lena C & Isope P (2013). Clusters of cerebellar Purkinje cells control their afferent climbing fiber discharge. *Proc Natl Acad Sci U S A* **110**, 16223–16228.

Coesmans M, Weber JT, De Zeeuw CI & Hansel C (2004). Bidirectional parallel fiber plasticity in the cerebellum under climbing fiber control. *Neuron* **44**, 691–700.

Coultrap SJ & Bayer KU (2012). CaMKII regulation in information processing and storage. *Trends Neurosci* **35**, 607–618.

Davie JT, Clark BA & Häusser M (2008). The origin of the complex spike in cerebellar Purkinje cells. *J Neurosci* **28**, 7599–7609.

Dean P, Porrill J, Ekerot CF & Jörntell H (2010). The cerebellar microcircuit as an adaptive filter: experimental and computational evidence. *Nat Rev Neurosci* **11**, 30–43.

De Gruijl JR, Hoogland TM & De Zeeuw CI (2014). Behavioral correlates of complex spike synchrony in cerebellar microzones. *J Neurosci* **34**, 8937–8947.

Ding F, O'Donnell J, Xu Q, Kang N, Goldman N & Nedergaard M (2016). Changes in the composition of brain interstitial ions control the sleep-wake cycle. *Science* **352**, 550–555.

Ebner TJ & Bloedel JR (1981). Role of climbing fiber afferent input in determining responsiveness of Purkinje cells to mossy fiber inputs. *J Neurophysiol* **45**, 962–971.

Eccles J, Llinás R & Sasaki K (1964). Excitation of cerebellar Purkinje cells by the climbing fibres. *Nature* **203**, 245–246.

Ekerot CF & Kano M (1989). Stimulation parameters influencing climbing fibre induced long-term depression of parallel fiber sysnapses. *Neurosci Res* **6**, 264–268.

Elgersma Y, Fedorov NB, Ikonen S, Choi ES, Elgersma M, Carvalho OM, Giese KP & Silva AJ (2002). Inhibitory autophosphorylation of CaMKII controls PSD association, plasticity, and learning. *Neuron* **36**, 493–505.

Freeman JH & Steinmetz AB (2011). Neural circuitry and plasticity mechanisms underlying delay eyeblink conditioning. *Learn Mem* **18**, 666–677.

Freeman JH (2015). Cerebellar learning mechanisms. *Brain Res* **1621**, 260–269.

Gallistel CR & Matzel LD (2013). The neuroscience of learning: beyond the Hebbian synapse. *Annu Rev Psychol* **64**, 169–200.

Gao Z, van Beugen BJ & De Zeeuw CI (2012). Distributed synergistic plasticity and cerebellar learning. *Nat Rev Neurosci* **13**, 619–635.

Gautier JC & Blackwood W (1961). Enlargement of the inferior olivary nucleus in association with lesions of the central tegmental tract or dentate nucleus. *Brain* **84**, 341–361.

Grundy D (2015). Principles and standards for reporting animal experiments in The Journal of Physiology and Experimental Physiology. *J Physiol* **593**, 2547–2549.

Han VZ, Zhang Y, Bell CC & Hansel C (2007). Synaptic plasticity and calcium signaling in Purkinje cells of the central cerebellar lobes of mormyrid fish. *J Neurosci* **27**, 13499–13512.

Hansel C & Linden DJ (2000). Long-term depression of the cerebellar climbing fiber-Purkinje neuron synapse. *Neuron* **26**, 473–482.

Hansel C, Linden DJ & D'Angelo E (2001). Beyond parallel fiber LTD: the diversity of synaptic and non-synaptic plasticity in the cerebellum. *Nat Neurosci* **4**, 467–475.

Hansel C, de Jeu M, Belmeguenai A, Houtman SH, Buitendijk GH, Andreev D, De Zeeuw CI & Elgersma Y (2006). αCaMKII is essential for cerebellar LTD and motor learning. *Neuron* **51**, 835–843.

Hartell NA (1996). Strong activation of parallel fibers produces localized calcium transients and a form of LTD that spreads to distant synapses. *Neuron* **16**, 601–610.

Heinemann U, Lux HD & Gutnick MJ (1977). Extracellular free calcium and potassium during paroxysmal activity in the cerebral cortex of the cat. *Exp Brain Res* **27**, 237–243.

Ito M, Sakurai M & Tongroach P (1982). Climbing fibre induced depression of both mossy fibre responsiveness and glutamate sensitivity of cerebellar Purkinje cells. *J Physiol* **324**, 113–134.

Ito M & Kano M (1982). Long-lasting depression of parallel fiber-Purkinje cell transmission induced by conjunctive stimulation of parallel fibers and climbing fibers in the cerebellar cortex. *Neurosci Lett* **33**, 253–258.

Johansson F, Jirenhed DA, Rasmussen A, Zucca R & Hesslow G (2014). Memory trace and timing mechanism localized to cerebellar Purkinje cells. *Proc Natl Acad Sci U S A* **111**, 14930–14934.

Kakegawa W, Katoh A, Narumi S, Miura E, Motohashi J, Takahashi A, Kohda K, Fukazawa Y, Yuzaki M & Matsuda S (2018). Optogenetic control of synaptic AMPA receptor endocytosis reveals roles of LTD in motor learning. *Neuron* **99**, 985–998.

Kawaguchi SY & Hirano T (2013). Gating of long-term depression by Ca^{2+}/calmodulin-dependent protein kinase II through enhanced cGMP signaling in cerebellar Purkinje cells. *J Physiol* **591**, 1707–1730.

Keating JG & Thach WT (1995). Nonclock behavior of inferior olive neurons: interspike interval of Purkinje cell complex spike discharge in the awake behaving monkey is random. *J Neurophysiol* **73**, 1329–1340.

Kitamura K & Häusser M (2011). Dendritic calcium signaling triggered by spontaneous and sensory-evoked climbing fiber input to cerebellar Purkinje cells in vivo. *J Neurosci* **31**, 10847–10858.

Konnerth A, Dreessen J & Augustine GJ (1992). Brief dendritic calcium signals initiate long-lasting synaptic depression in cerebellar Purkinje cells. *Proc Natl Acad Sci U S A* **89**, 7051–7055.

Lamarre Y (1984). Animal models of physiological, essential, and parkinsonian-like tremors. In: *Movement Disorders: Tremor*, eds. Findlay LJ & Capildeo R, pp 183–194. Oxford University Press, New York, NY.

Lang EJ, Sugihara I, Welsh JP & Llinás R (1999). Patterns of spontaneous purkinje cell complex spike activity in the awake rat. *J Neurosci* **19**, 2728–2739.

Lev-Ram V, Wong ST, Storm DR & Tsien RY (2002). A new form of cerebellar long-term potentiation is postsynaptic and depends on nitric oxide but not cAMP. *Proc Natl Acad Sci U S A* **99**, 8389–8393.

Llinás R (1984). Rebound excitation as the physiological basis for tremor: a biophysical study of the oscillatory properties of mammalian central neurons in vitro. In: *Movement Disorders: Tremor*, eds. Findlay LJ & Capildeo R, pp 165–182. Oxford Univesrity Press, New York, NY.

Llinás R (2011). Cerebellar motor learning versus cerebellar motor timing: the climbing fibre story. *J Physiol* **589**, 3423–3432.

Margrie TW, Brecht M & Sakmann B (2002). In vivo, low-resistance, whole-cell recordings from neurons in the anaesthetized and awake mammalian brain. *Pflügers Arch* **444**, 491–498.

Marquez-Ruiz J & Cheron G (2012). Sensory stimulation-dependent plasticity in the cerebellar cortex of alert mice. *PLoS ONE* **7**, e36184.

Marr D (1969). Theory of cerebellar cortex. *J Physiol* **202**, 437–455.

Maruta J, Hensbroek RA & Simpson JI (2007). Intraburst and interburst signaling by climbing fibers. *J Neurosci* **27**, 11263–11270.

Mathy A, Ho SSN, Davie JT, Duguid IC, Clark BA & Häusser M (2009). Encoding of oscillations by axonal bursts in inferior olive neurons. *Neuron* **62**, 388–399.

Najafi F, Giovannucci A, Wang SS-H & Medina JF (2014*a*). Sensory-driven enhancement of calcium signals in individual Purkinje cell dendrites of awake mice. *Cell Rep* **6**, 792–798.

Najafi F, Giovannucci A, Wang SS-H & Medina JF (2014*b*). Coding of stimulus strength via analog calcium signals in Purkinje cell dendrites of awake mice. *eLife* **3**, e03663.

Nicholson C, ten Bruggencate G, Stockle H & Steinberg R (1978). Calcium and potassium changes in extracellular microenvironment of cat cerebellar cortex. *J Neurophysiol* **41**, 1026–1039.

Ohmae S & Medina JF (2015). Climbing fibers encode a temporal-difference prediction error during cerebellar learning in mice. *Nat Neurosci* **18**, 1798–1803.

Ohtsuki G, Piochon C, Adelman JP & Hansel C (2012). SK2 channel modulation contributes to compartment-specific dendritic plasticity in cerebellar Purkinje cells. *Neuron* **75**, 108–120.

Ohtsuki G & Hansel C (2018). Synaptic potential and plasticity of an SK2 channel gate regulate spike burst activity in cerebellar Purkinje cells. *iScience* **1**, 49–54.

Oscarsson O (1980). Functional organization of olivary projection to the cerebellar anterior lobe. In: *The Inferior Olivary Nucleus: Anatomy and Physiology*, ed. Courville J, de Montigny C & Lamarre Y, pp. 279–289. Raven, New York, NY.

Ozden I, Sullivan MR, Lee HM & Wang SS-H (2009). Reliable coding emerges from co-activation of climbing fibers in microbands of cerebellar Purkinje neurons. *J Neurosci* **29**, 10463–10473.

Piochon C, Titley HK, Simmons DH, Grasselli G, Elgersma Y & Hansel C (2016). Calcium threshold shift enables frequency-independent control of plasticity by an instructive signal. *Proc Natl Acad Sci U S A* **113**, 13221–13226.

Rasmussen A, Jirenhed DA, Zucca R, Johansson F, Svensson P & Hesslow G (2013). Number of spikes in climbing fibers determines the direction of cerebellar learning. *J Neurosci* **33**, 13436–13440.

Rowan MJ, Bonnan A, Zhang K, Amat SB, Kikuchi C, Taniguchi H, Augustine GJ & Christie JM (2018). Graded control of climbing fiber-mediated plasticity and learning by inhibition in the cerebellum. *Neuron* **99**, 999–1015.

Safo P & Regehr WG (2008). Timing dependence of the induction of cerebellar LTD. *Neuropharmacology* **54**, 213–218.

Santamaria F, Wils S, De Schutter E & Augustine GJ (2006). Anomalous diffusion in Purkinje cell dendrites caused by spines. *Neuron* **52**, 635–648.

Sarkisov DV & Wang SS-H (2008). Order-dependent coincidence detection in cerebellar Purkinje neurons at the inositol trisphosphate receptor. *J Neurosci* **28**, 133–142.

Schmidt H, Brown EB, Schwaller B & Eilers J (2003). Diffusional mobility of parvalbumin in spiny dendrites of cerebellar Purkinje neurons quantified by fluorescence recovery after photobleaching. *Biophys J* **84**, 2599–2608.

Schmidt H, Kunerth S, Wilms C, Strotmann R & Eilers J (2007). Spino-dendritic cross-talk in rodent Purkinje neurons mediated by endogenous Ca^{2+}-binding proteins. *J Physiol* **581**, 619–629.

Schonewille M, Gao Z, Boele HJ, Vinueza Veloz MF, Amerika WE, Simek AA, De Jeu MT, Steinberg JP, Takamiya K, Hoebeek FE, Linden DJ, Huganir RL & De Zeeuw CI (2011). Reevaluating the role of LTD in cerebellar motor learning. *Neuron* **70**, 43–50.

Suvrathan A, Payne HL & Raymond JL (2016). Timing rules for synaptic plasticity matched to behavioral function. *Neuron* **92**, 959–967.

Tanaka K, Khiroug L, Santamaria F, Doi T, Ogasawara H, Ellis-Davies GC, Kawato M & Augustine GJ (2007). Ca^{2+} requirements for cerebellar long-term synaptic depression: role for a postsynaptic leaky integrator. *Neuron* **54**, 787–800.

Ten Brinke MM, Boele HJ, Spanke JK, Potters JW, Kornysheva K, Wulff P, Ijpelaar AC, Koekkoek SK & De Zeeuw CI (2015). Evolving models of Pavlovian conditioning: cerebellar cortical dynamics in awake behaving mice. *Cell Rep* **13**, 1977–1988.

Ten Brinke MM, Boele HJ & De Zeeuw CI (2019). Conditioned climbing fiber responses in cerebellar cortex and nuclei. *Neurosci Lett* **688**, 26–36.

Thach WT (1968). Discharge of Purkinje and cerebellar nuclear neurons during rapidly alternating arm movements in the monkey. *J Neurophysiol* **31**, 785–797.

Titley HK, Brunel N & Hansel C (2017). Toward a neurocentric view of learning. *Neuron* **95**, 19–32.

Titley HK, Watkins GV, Lin C, Weiss C, McCarthy M, Disterhoft JF & Hansel C (2018). Intrinsic excitability increase in cerebellar purkinje cells following delay eyeblink conditioning in mice. *BioRxiv* https://doi.org/10.1101/306639.

Van der Giessen RS, Koekkoek SK, van Dorp S, De Gruijl JR, Cupido A, Khosrovani S, Dortland B, Wellershaus K, Degen J, Deuchars J, et al. (2008). Role of olivary electrical coupling in cerebellar motor learning. *Neuron* **58**, 599–612.

Wang SS-H, Denk W & Häusser M (2000). Coincidence detection in single dendritic spines mediated by calcium release. *Nat Neurosci* **3**, 1266–1273.

Welsh JP, Lang EJ, Sugihara I & Llinás R (1995). Dynamic organization of motor control within the olivocerebellar system. *Nature* **374**, 453–457.

Welsh JP, Yamaguchi H, Zeng XH, Kojo M, Nakada Y, Takagi A, Sugimori M & Llinás RR (2005). Normal motor learning during pharmacological prevention of Purkinje cell long-term depression. *Proc Natl Acad Sci U S A* **102**, 17166–17171.

Wetmore DZ, Jirenhed D-A, Rasmussen A, Johansson F, Schnitzer MJ & Hesslow G (2014). Bidirectional plasticity of Purkinje cells matches temporal features of learning. *J Neurosci* **34**, 1731–1737.

Witter L, Canto CB, Hoogland TM, de Gruijl JR & De Zeeuw CI (2013). Strength and timing of motor responses mediated by rebound firing in the cerebellar nuclei after Purkinje cell activation. *Front Neural Circuits* **7**, 133.

Yamaguchi K, Itohara S & Ito M (2016). Reassessment of long-term depression in cerebellar Purkinje cells in mice carrying mutated GluA2 C terminus. *Proc Natl Acad Sci U S A* **113**, 10192–10197.

Yang Y & Lisberger SG (2014). Purkinje-cell plasticity and cerebellar motor learning are graded by complex-spike duration. *Nature* **510**, 529–532.

Additional information

Competing interests

The authors declare that they have no competing interests.

Author contributions

HKT, CH, and SS-HW designed the experiments. HKT, MK and DHS conducted the experiments and analysed data. HKT, SS-HW and CH wrote the manuscript. All authors have approved the final version of the manuscript submitted for publication. The authors agree to be accountable for all aspects of the work in ensuring that questions related to the accuracy or integrity of any part of the work are appropriately investigated and resolved. All persons designated as authors qualify for authorship, and all those who qualify for authorship are listed.

Funding